SAND2020-13334C

Sandia National Laboratories

Progress on an IMEX Multifluid EM Plasma Formulation for Challenging Fusion Related Applications

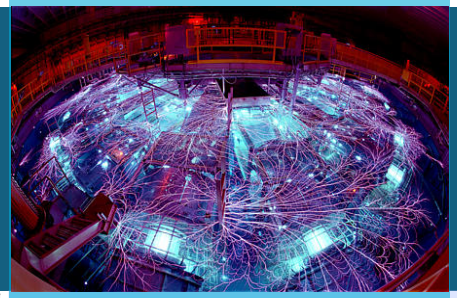

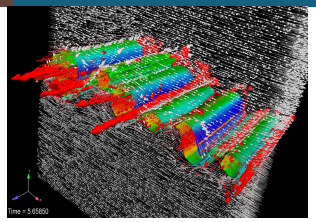

Hydro-Magnetic Kelvin-Helmholtz Instability

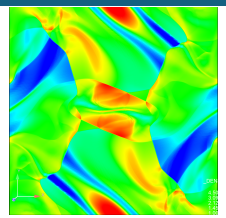

Orszag-Tang Shock MHD

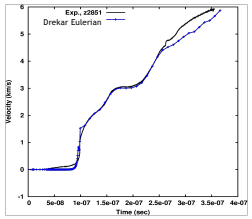

1D Al Flyer Plate VISAR Experiment. vs. Sim.

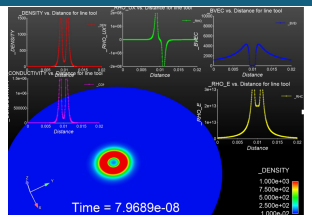

2D Gas Z-pinch Implosion

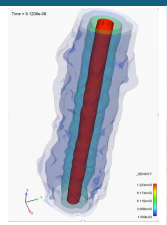

3D Gas Z-pinch Implosion

J. N. Shadid, M. M. Crockatt,. S. Conde, T. M. Smith, R. Pawlowski, I. Tomas, A. Rappaport, S. Mabuza (Clemson)

Office of Science

- Advanced Scientific Computing Research
- Fusion Energy Sciences

U.S. DEPARTMENT OF ENERGY NNSA

Sandia National Laboratories is a multimission laboratory managed and operated by National Technology and Engineering Solutions of Sandia LLC, a wholly owned subsidiary of Honeywell International Inc. for the U.S. Department of Energy's National Nuclear Security Administration under contract DE-NA0003525.

Outline

- General Scientific and Mathematical/Computational Motivation
- Comments on Multiple-time-scale Plasma Systems
  - Magnetic Confinement Fusion: Tokamak Device
  - Magnetic Inertial Fusion: Z-pinch (not discussed but a strong motivation)
- Brief Description of Continuum Multifluid EM PDE Model
- Very Brief Illustration of Scalable Solution Methods
  - Multifluid EM Plasmas (Approximate Block Factorization Preconditioners, AMG block solvers)
- Demonstration and Evaluation
  - Temporal/Spatial Discretization of MHD/Multifluid EM Plasma Models (AFC CG Galerkin);
  - Preliminary Results for Multifluid EM Plasma Model Related Applications
    - Magnetic Confinement Fusion: Tokamak Disruption Mitigation (neutral gas injection)
    - Magnetic Inertial Fusion: Ar gas puff Z-pinch
- Concluding Remarks

Motivation: Science/Technology

MHD and multifluid EM plasma models are used to study important multiple-time/ length-scale multiphysics plasma physics systems

- **Astrophysics and Planetary-physics:**
  - **Magnetic reconnection, instabilities,**
  - **Solar flares, Coronal Mass Ejections.**
  - **Earth's magnetospheric sub-storms,**
  - **Aurora, Planetary-dynamos.**
- **Fusion & High Energy Density Physics:**
  - **Magnetic Confinement [MCF] (e.g. ITER),**
  - **Inertial Confinement [ICF] (e.g. Z-pinch, NIF).**

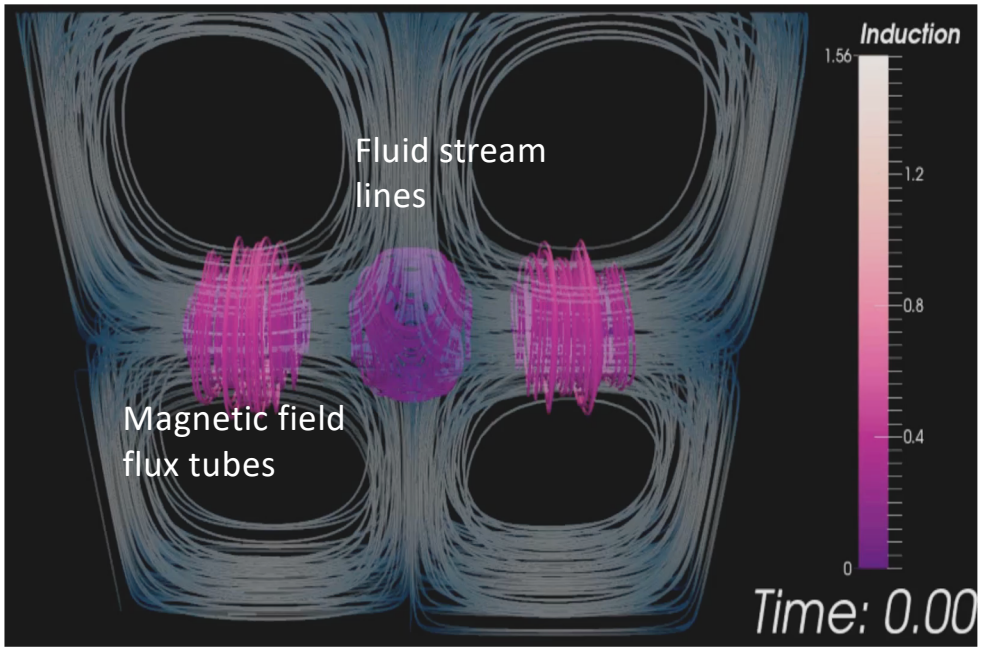

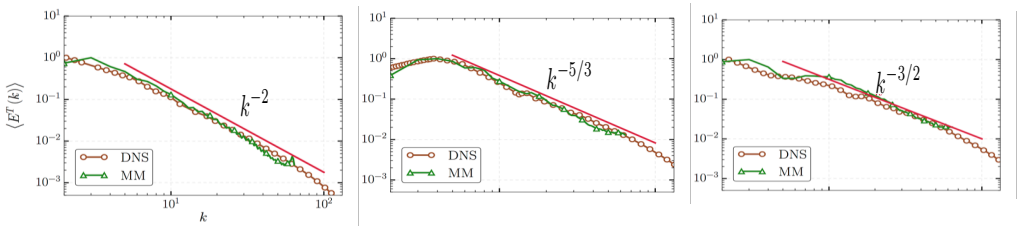

MHD VMS–LES MHD Turbulence Modeling Taylor-Green Vortex Decay. Illustration of non-universality of total MHD energy turbulent decay spectrum [with D. Sondak (Harvard), A. Oberai (USC)]

E.g. Multiple-time-scale Multiphysics System: Magnetic Confinement Fusion

Goal for Fusion Device:

- Attempt is to achieve temperature of ~100M deg K (6x Sun temp.) ,
- Energy confinement times O(1) min. are desired.
- Understanding and controlling instabilities/disruptions in plasma confinement is critical

Strong external magnetic fields used for:

- Resistive heating of the plasma (along with RF-EM waves, ..)
- Confinement of the hot plasma to keep it from striking the wall
  - Plasma disruptions can cause break of confinement, huge plasma thermal energy loss, and discharge of very large electrical currents (~20MA) to surface and damage the device.
  - ITER can sustain only a limited number of significant disruptions, O(1 – 5).

(ITER)

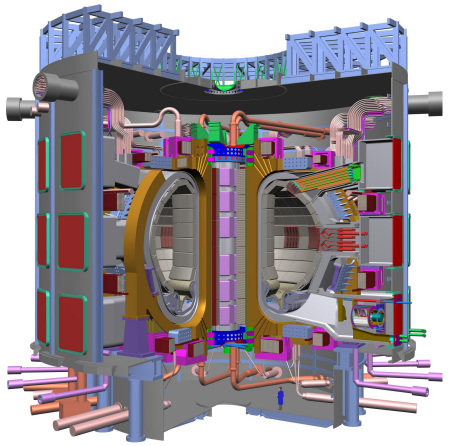

International Thermonuclear Experimental Reactor [under construction, Cadarache facility France]

E.g. Multiple-time-scale Multiphysics System: Magnetic Confinement Fusion (MCF)

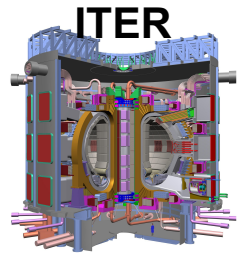

MCF Devices (e.g. ITER) are characterized by large-range of time and length-scales

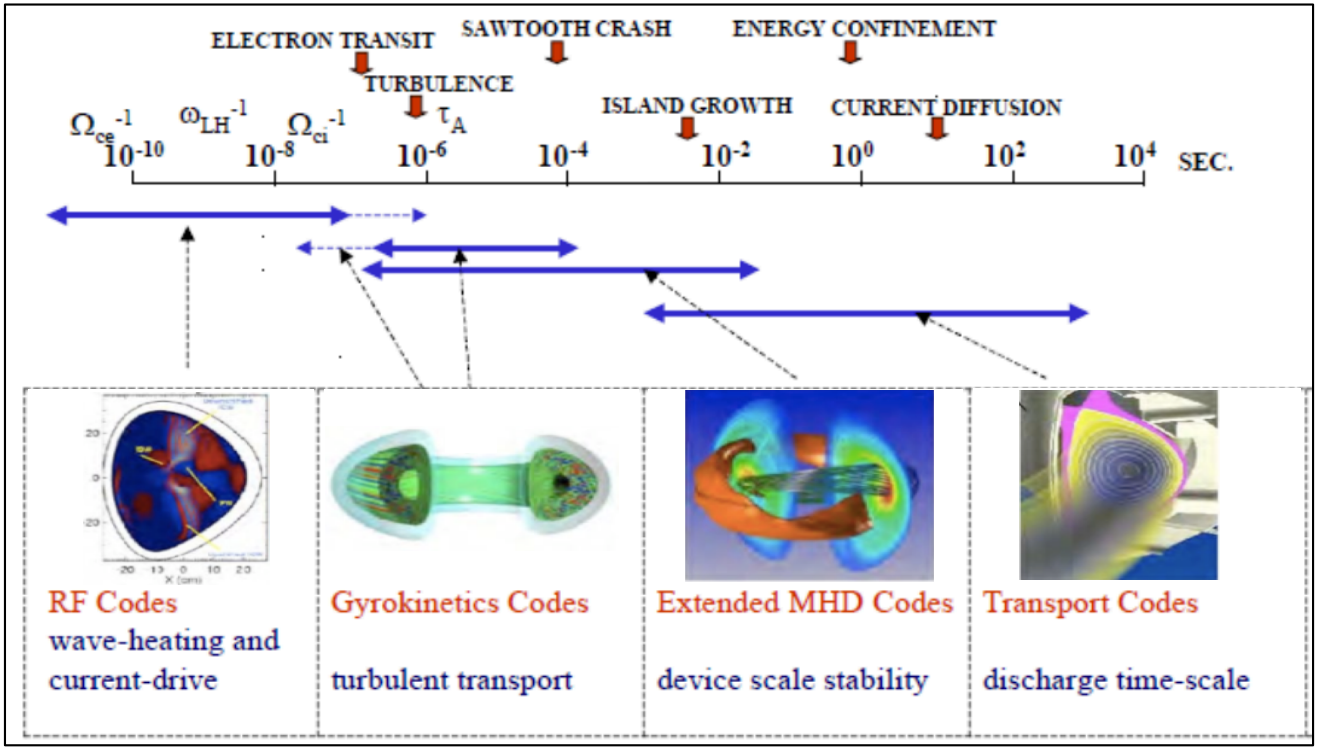

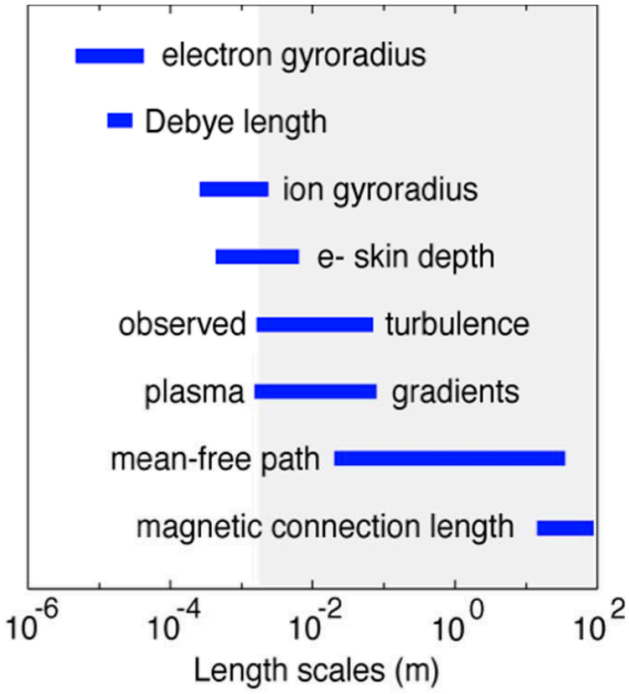

DOE Office of Science ASCR/OFES Reports: Fusion Simulation Project Workshop Report, 2007, Integrated System Modeling Workshop 2015

Multifluid EM Plasma Model

Density	$\partial_t \rho_s + \nabla \cdot (\rho_s \mathbf{u}_s) = -\rho_s n_e (I_s + R_s) + m_s n_e (n_{s-1} I_{s-1} + n_{s+1} R_{s+1})$
Momentum	$\partial_t (\rho_s \mathbf{u}_s) + \nabla \cdot (\rho_s \mathbf{u}_s \otimes \mathbf{u}_s + p_s \underline{\mathbf{I}} + \underline{\boldsymbol{\Pi}}_s) = q_s n_s (\mathbf{E} + \mathbf{u}_s \times \mathbf{B}) + \sum_{t \neq s} \alpha_{s;t} \rho_s \rho_t (\mathbf{u}_t - \mathbf{u}_s)$ $-\rho_s \mathbf{u}_s n_e (I_s + R_s) + \frac{m_s}{m_{s-1}} n_e \rho_{s-1} \mathbf{u}_{s-1} I_{s-1} + (n_e \rho_{s+1} \mathbf{u}_{s+1} + n_{s+1} \rho_e \mathbf{u}_e) R_{s+1}$
Energy	$\partial_t \mathcal{E}_s + \nabla \cdot [(\mathcal{E}_s + p_s) \mathbf{u}_s + \mathbf{u}_s \cdot \underline{\boldsymbol{\Pi}}_s + \mathbf{h}_s] = q_s n_s \mathbf{u}_s \cdot \mathbf{E} + \sum_{t \neq s} \frac{\alpha_{s;t} \rho_s \rho_t}{m_s + m_t} [A_{s;t} k_B (T_t - T_s) + m_t (\mathbf{u}_t - \mathbf{u}_s)^2]$ $-\mathcal{E}_s n_e (I_s + R_s) + \frac{m_s}{m_{s-1}} n_e \mathcal{E}_{s-1} I_{s-1} + (n_e \mathcal{E}_{s+1} + n_{s+1} \mathcal{E}_e) R_{s+1}$
Charge and Current	$q = \sum_s q_s n_s$ $\quad$ $\mathbf{J} = \sum_s q_s n_s \mathbf{u}_s$
Maxwell's Equations	$\frac{1}{c^2} \partial_t \mathbf{E} - \nabla \times \mathbf{B} + \mu_0 \mathbf{J} = \mathbf{0}$ $\quad$ $\nabla \cdot \mathbf{E} = \frac{q}{\epsilon_0}$ $\partial_t \mathbf{B} + \nabla \times \mathbf{E} = \mathbf{0}$ $\quad$ $\nabla \cdot \mathbf{B} = 0$

Other work on mulitfluid formulations, solution algorithms:

See e.g.
Abgral et. al.;
Barth;
Kumar et. al.;
Laguna et. al.;
Rossmanith et. al.;
Shumlak et. al.;
B. Srinivasan et. al.;

1. Flexible and extensible multiphysics PDE solver framework (**Drekar**) can accommodate arbitrary numbers of species.
2. Nodal FE or structure-preserving FE discretizations (edge, face, etc.).
3. Stable and accurate AFC local bounds preserving CG FE methods.
4. IMEX capabilities for handling disparate time scales (eg., large plasma/cyclotron freq., EM CFL, etc.).
5. Robust and scalable linear and nonlinear solvers for CG/structure preserving methods

   $\Rightarrow$ Newton-Krylov with physics-based block decomposition preconditioning; enabling optimal H(curl) and H(grad) multilevel subsystem solvers.

Demonstration of scalable physics-based preconditioners / solvers for multifluid (ion-electron) EM plasmas: 3D Gaussian high pressure initial condition for isentropic ion-acoustic wave propagation

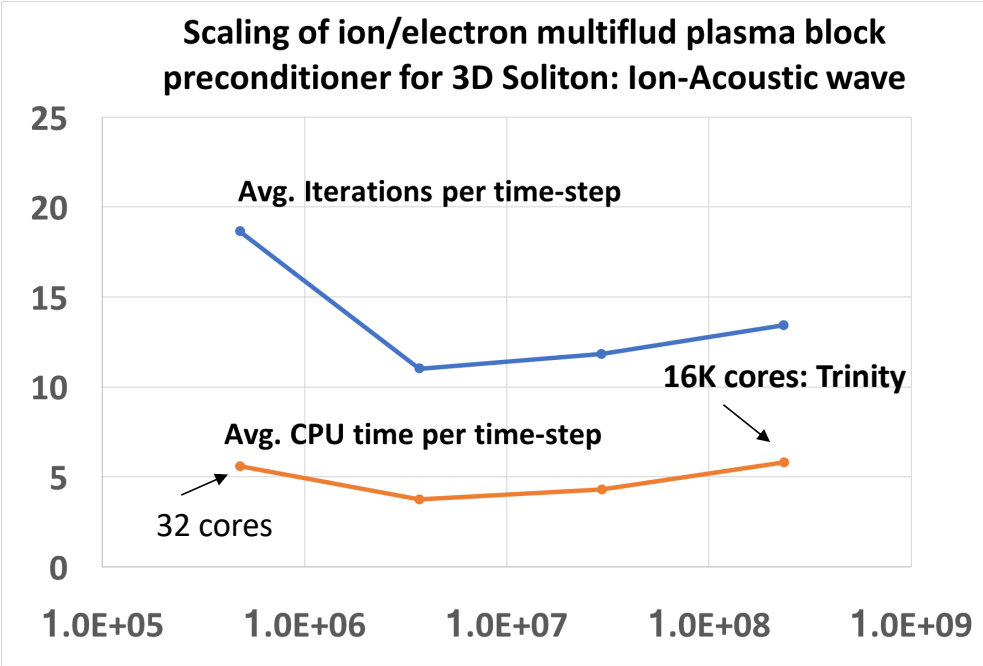

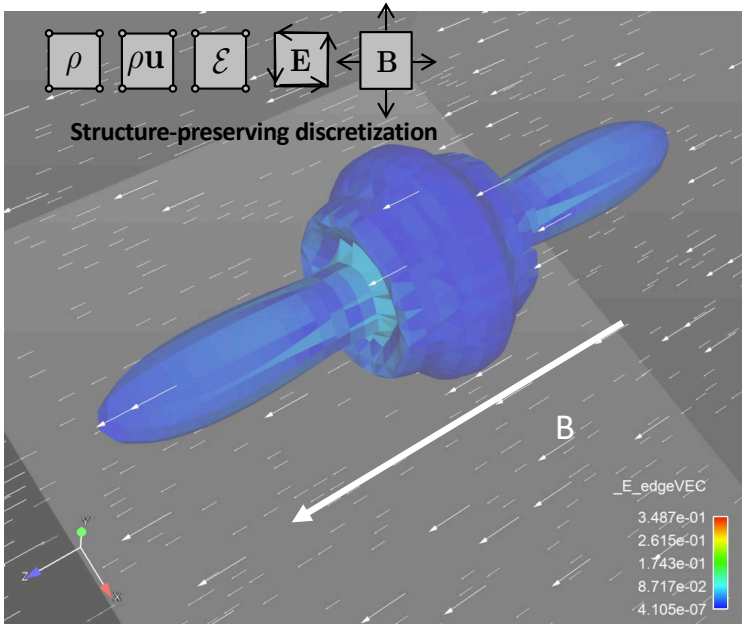

Iso-surface of ion density colored by electric field magnitude

Drekar has been demonstrated to weak scale to 1M+ cores for MHD

Lin, S, ….. …et. al., JCAM 2019

Ref others

Crockatt, Shadid, Multifluid Plasma Models for Drekar, Sand Report in Progress, 2020

Miller, Cyr, Shadid, Kramer, Phillips, Conde, Pawlowski, IMEX and exact sequence discretization of the multi-fluid plasma model. JCP, 2019

Kramer, Cyr, Miller, Phillips , Radtke, Robinson, Shadid A Plasma Modeling Hierarchy and Verification Approach, Sand Report 2020-3576, 2020

Phillips, Shadid, Cyr, and Miller, "Enabling scalable multifluid plasma simulations through block preconditioning," LNCSE, 2020.

Demonstration / Verification of Implicit Solution for Longitudinal Electron Plasma (LEP) Oscillation with a Highly Under-resolved TEM Wave (SDIRK22)

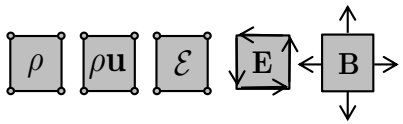

Nodal FE Hydro and Structure-preserving discretization for EM

$$\Delta t = 0.1 * \tau_{\omega_{pe}} \approx 10^4 * \tau_{EM} \quad \text{(on 3200 fine mesh)}$$

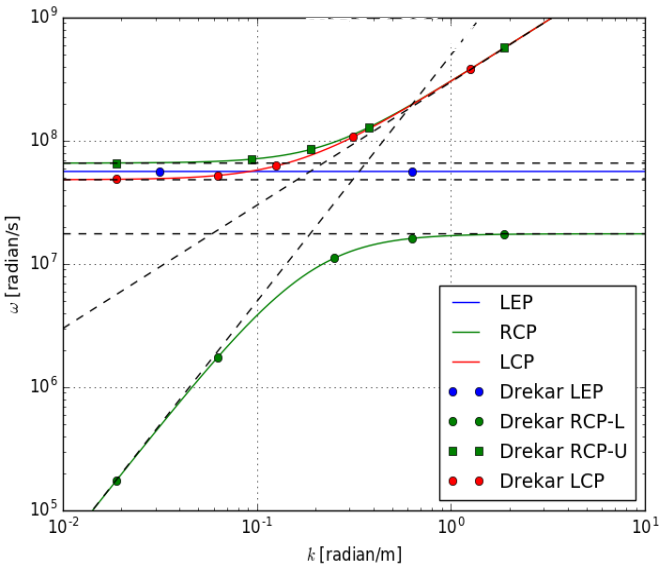

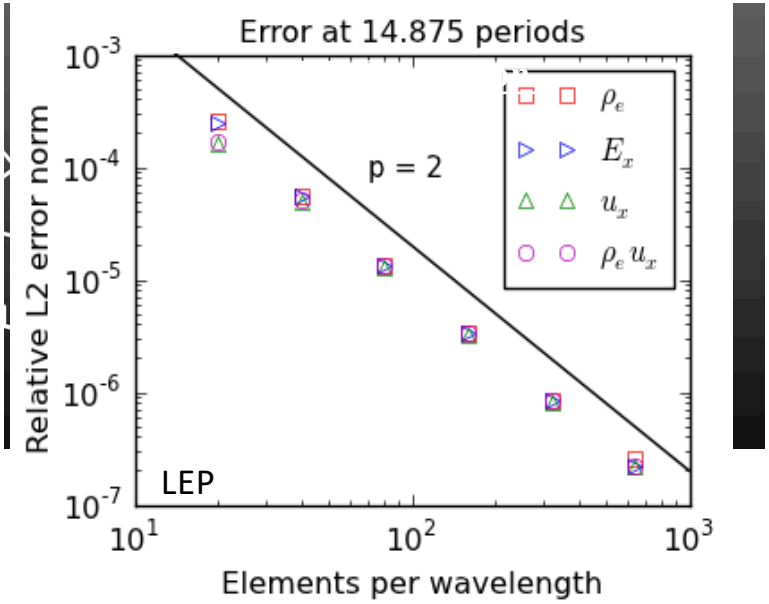

LEP: Longitudinal Electron Plasma Wave
RCP: Right Hand Circularly Polarized Wave
LCP: Left Hand Circularly Polarized Wave
(Cold plasma)

Verification effort with Niederhaus, Radtke, Bettencourt, Cartwright, Kramer, Robinson and ATDM EMPIRE Team

Robustness and Accuracy: Asymptotic IMEX Solution of Full Multifluid EM Plasma Model in MHD Limit (Visco-Resistive Alfven Wave)

Implicit L-stable and IMEX SSP/L-stable time integration and block preconditioners enable solution of multifluid EM plasma model in the asymptotic resistive MHD limit.

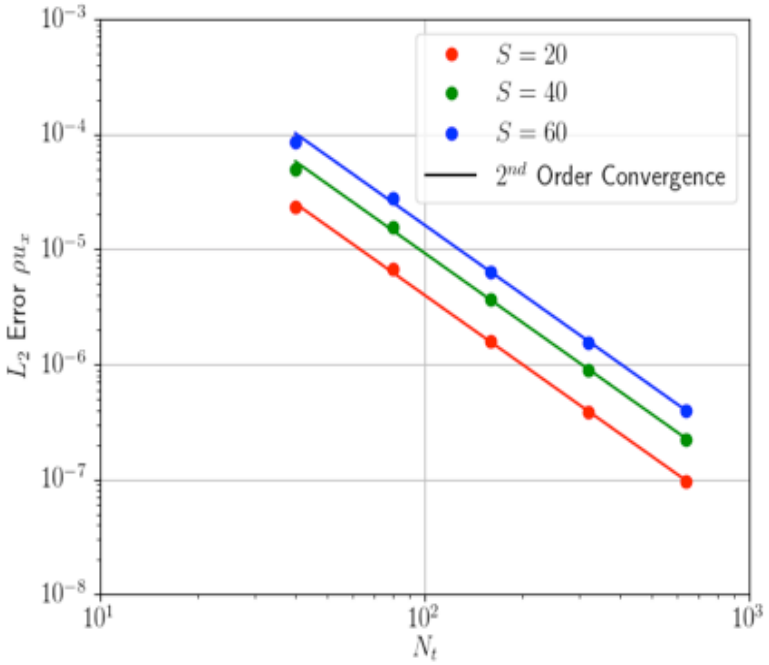

Accuracy in MHD limit (IMEX)

Plasma Scales for S = 60		
	Electrons	Ions
$\omega_p \Delta t$	10^7 - 10^9	10^6 - 10^7
$\omega_c \Delta t$	10^6 - 10^7	10^3 - 10^4
$\nu_{\alpha\beta} \Delta t$	10^{10} - 10^{11}	10^7 - 10^8
$\nu_S \Delta t / \Delta x$	10^{-2}	10^{-4}
$u \Delta t / \Delta x$	10^{-4}	10^{-4}
$\mu \Delta t / \rho \Delta x^2$	10^{-1} - 10^{1}	10^{-2} - 10^{0}
$c \Delta t / \Delta x$	10^2	

IMEX terms: implicit/explicit

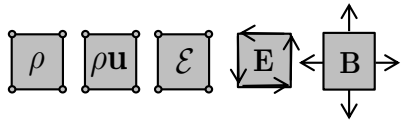

Nodal FE Hydro and Structure-preserving discretization for EM

Implicitly overstepping stiff modes, not controlling accuracy, can make an intractable explicit computation – tractable with IMEX methods.

Overstepping fast time scales is both stable and accurate. The inclusion of a resistive operator adds dissipation to the electron dynamics on top of the L-stable time integrator.

S. T. Miller, E. C. Cyr, JS, R. M. J. Kramer, E. G. Phillips, S. Conde, R. P. Pawlowski, IMEX and exact sequence discretization of the multi-fluid plasma model. In press for JCP

Stabilization based on Hyperbolic System Solvers: Discrete Algebraic Flux Correction [AFC] (follows D. Kuzmin et. al.)

$$\frac{\partial \mathbf{U}}{\partial t} + \nabla \cdot \mathbf{F}(\mathbf{U}) = \mathbf{S}(\mathbf{U})$$

Resistive MHD

$$\mathbf{U} = [\rho, \rho\mathbf{u}, \rho\mathcal{E}, \mathbf{B}]^T; \quad \mathbf{S} = \mathbf{0}$$

$$\mathbf{F} = \begin{bmatrix} \rho\boldsymbol{v} & \\ \rho\boldsymbol{v}\otimes\boldsymbol{v} + pI - \boldsymbol{T}_M & -\boldsymbol{T} \\ \boldsymbol{v}\cdot((\rho E + p)I - \boldsymbol{T}_M) & -\boldsymbol{v}\cdot\boldsymbol{T} + \boldsymbol{q} - \frac{\eta}{\mu_0}\boldsymbol{B}\cdot(\nabla\boldsymbol{B} - (\nabla\boldsymbol{B})^T) \\ \boldsymbol{B}\otimes\boldsymbol{v} - \boldsymbol{v}\otimes\boldsymbol{B} & -\frac{\eta}{\mu_0}(\nabla\boldsymbol{B} - (\nabla\boldsymbol{B})^T) \end{bmatrix}$$

Multifluid EM Plasma (for multiple species, s; shown in divergence form)

$$\mathbf{U} = [\{(\mathbf{U}_s),\ \forall s \in \Lambda\}, \mathbf{U}_{EM}]^T.\ \mathbf{U}_s = [\rho_s, \rho_s\mathbf{u}_s, \rho_s\mathcal{E}_s]^T, \text{ and } \mathbf{U}_{EM} = [\mathbf{B}, \mathbf{E}]^T$$

$$\mathbf{F} = \begin{bmatrix} \mathbf{F}_1(\mathbf{U}_1) \\ ..... \\ \mathbf{F}_{N_s}(\mathbf{U}_{N_s}) \\ \mathbf{F}_{EM}(\mathbf{U}_{EM}) \end{bmatrix};\ \mathbf{F}_s(\mathbf{U}_s) = \begin{bmatrix} \rho_s\mathbf{u}_s \\ \rho_s\mathbf{u}_s\otimes\mathbf{u}_s + p_sI \\ (\rho\mathcal{E}_s + p_s)\mathbf{u}_s \end{bmatrix};\quad \mathbf{F}_{EM}(\mathbf{U}_{EM}) = \begin{bmatrix} \mathcal{T}(\mathbf{E}) \\ -c^2\mathcal{T}(\mathbf{B}) \end{bmatrix};$$

$$\mathcal{T}(\mathbf{w}) = \begin{bmatrix} 0 & w_z & -w_y \\ -w_z & 0 & w_x \\ w_y & -w_x & 0 \end{bmatrix}.$$

$$\mathbf{S}(\mathbf{U}) = [\{(\mathbf{S}_s),\ \forall s \in \Lambda\}, \mathbf{S}_{EM}(\mathbf{U})]^T;\quad \mathbf{S}_s(\mathbf{U}) = \begin{bmatrix} 0 \\ \frac{q_s\rho_s}{m_s}(\mathbf{E} + \mathbf{u}_s\times\mathbf{B}) \\ \frac{q_s\rho_s}{m_s}\mathbf{u}_s\cdot\mathbf{E} \end{bmatrix},\quad \mathbf{S}_{EM}(\mathbf{U}) = \begin{bmatrix} \mathbf{0} \\ -\mu_0c^2\sum_s \frac{q_s\rho_s}{m_s}\mathbf{u}_s \end{bmatrix}.$$

AFC Solution: Orszag – Tang MHD Vortex Prb.; 1024x1024 mesh

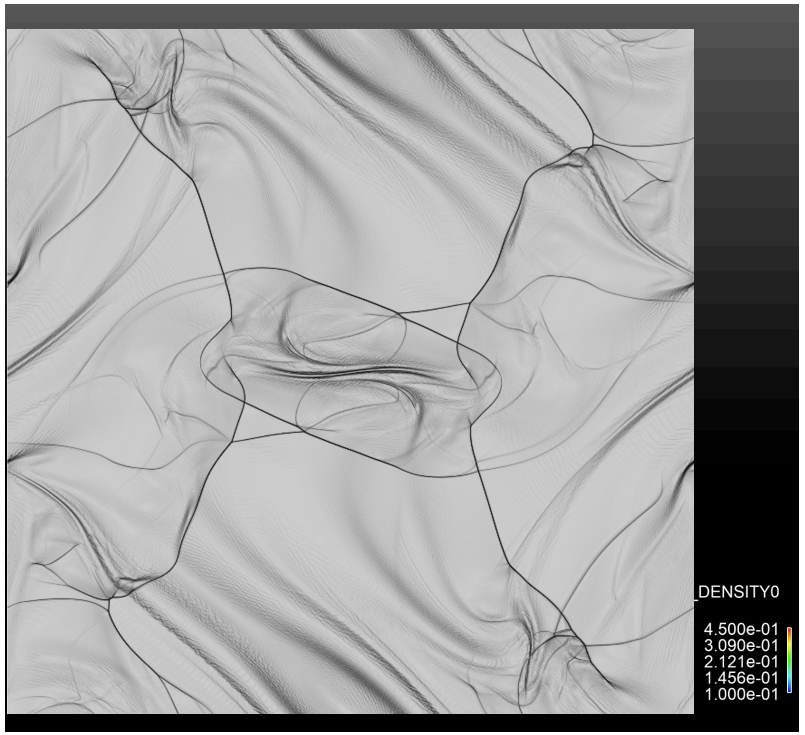

Mabuza, S, Kuzmin, JCP 2018
Mabuza, S, Cyr, Pawlowski, Kuzmin, JCP 2020

Semi-discrete AFC Stabilized System (Continuous Galerkin FE discretization) [See M. Crockatt talk for more details #2405]

$$\underbrace{\mathbf{M}_L \frac{d\mathbf{U}}{dt}}_{\text{Lumped Mass}} + \mathbf{K}(\mathbf{U}) + \mathbf{B}_{\mathbf{\Gamma}}(\mathbf{U}) + \underbrace{\mathbf{D}(\mathbf{U})\mathbf{U}}_{\text{Discrete dissipation operator}} - \sum_e \alpha_e \mathbf{F}^{(\mathbf{e})} = \mathbf{0}$$

Semi-discrete low-order representation

Limited difference of low-order to high-order flux

$$\alpha_e \in [0, 1]$$

Element correction factor blends low-order ($\alpha_e = 0$) with high-order ($\alpha_e = 1$)

Constructed from nodal variation limiters*.

$$\text{where } \mathbf{F}^{(e)} = (\mathbf{M}_L^{(e)} - \mathbf{M}_C^{(e)})\dot{\mathbf{U}}^{(e)} + \mathbf{D}^{(\mathbf{e})}(\mathbf{U}^{(\mathbf{e})})\mathbf{U}^{(\mathbf{e})}$$

Discrete dissipation of the low-order method ($[\mathbf{M}_C^{(e)} - \mathbf{M}_L^{(e)}]$, $\mathbf{D}^{(\mathbf{e})}$) is *conservative modification* (zero row/column sums) and is chosen to *bound maximum propagation speed of systems* (or sub-systems)

$$\mathbf{D} = \sum_e \mathbf{D}^{(e)}, \ \mathbf{D}^{(e)} = \{D_{ij}^{(e)}\}_{i,j}, \ D_{ij}^{(e)} = D_{ji}^{(e)}, \ D_{ii}^{(e)} = -\sum_{j \neq i} D_{ij}^{(e)}.$$

For scalar dissipation (Rusanov) $D_{ij}^{(e)} = d_{ij}^{(e)} I_{m \times m}$,

$$d_{ij}^{(e)} = \max\left\{ \|\boldsymbol{c}_{ji}^{(e)}\| \lambda_{\max}(\boldsymbol{U}_i, \boldsymbol{n}_{ji}^{(e)}), \|\boldsymbol{c}_{ij}^{(e)}\| \lambda_{\max}(\boldsymbol{U}_j, \boldsymbol{n}_{ij}^{(e)}) \right\}, \ j \neq i,$$

$$d_{ii}^{(e)} = -\sum_{j \neq i} d_{ij}^{(e)}, \ \boldsymbol{n}_{ij}^{(e)} = \frac{\boldsymbol{c}_{ij}^{(e)}}{\|\boldsymbol{c}_{ij}^{(e)}\|}, \ \boldsymbol{c}_{ij}^{(e)} = \int_{K_e} \nabla \phi_i \phi_j d\boldsymbol{x}, \text{ for each } K_e \in S_h.$$

Linearized hyperbolic system
*Local Extremum Diminishing (LED) for characteristic variable formulation**. Consistency of first order method: $O(h * \lambda_{max})$

**Kuzmin et. al. FCT books 2005, 2012; CMAME 2017;*
**Mabuza et. al., JCP 2018, 2020;*

Robustness and Accuracy: AFC - Ideal MHD

AFC local bounds preserving method:
Ideal MHD smooth Alfven wave convergence

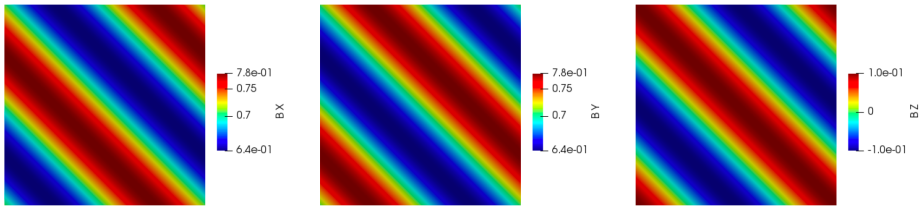

Figure 8: The smooth Aflven wave magnetic field profiles for the solution obtained when segregated limiting based on ρ is applied. The mesh has $\Delta x = \Delta y = \frac{1}{256}$. The time step is $\Delta t = 1.5625 \times 10^{-4}$.

Δx	Δt	L^1	EOC_1	L^2	EOC_2
$\frac{1}{8}$	5×10^{-3}	$9.56965103e-02$	–	$7.49845125e-02$	–
$\frac{1}{16}$	2.5×10^{-3}	$2.80237139e-02$	1.7718	$2.20141990e-02$	1.7681
$\frac{1}{32}$	1.25×10^{-3}	$7.22549121e-03$	1.9554	$5.67504738e-03$	1.9557
$\frac{1}{64}$	6.25×10^{-4}	$1.81897295e-03$	1.9899	$1.42867753e-03$	1.9899
$\frac{1}{128}$	3.125×10^{-4}	$4.55539220e-04$	1.9974	$3.57774759e-04$	1.9975
$\frac{1}{256}$	1.5625×10^{-4}	$1.13931076e-04$	1.9994	$8.94807819e-05$	1.9994

Table 12: The convergence rates for B_y in the smooth Alfven wave test when segregated limiting based on ρ is used.

AFC local bounds preserving method:

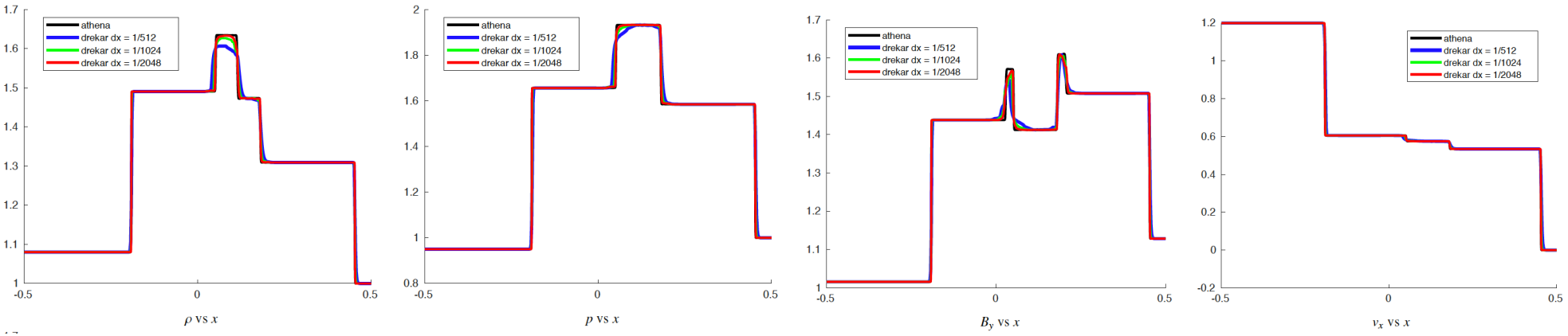

Mabuza, S, Kuzmin, JCP 2018
Mabuza, S, Cyr, Pawlowski, Kuzmin, JCP 2020

Robustness and Accuracy: AFC – Two-fluid EM Plasma (Brio-Wu and GEM Challenge)

Two-fluid Brio-Wu Problem

Resolved Two-fluid scales
Brio-Wu Problem
Two-fluid regime:

$$\hat{\mu} = \hat{\lambda}_D = \hat{r}_L = 10^{-2}$$

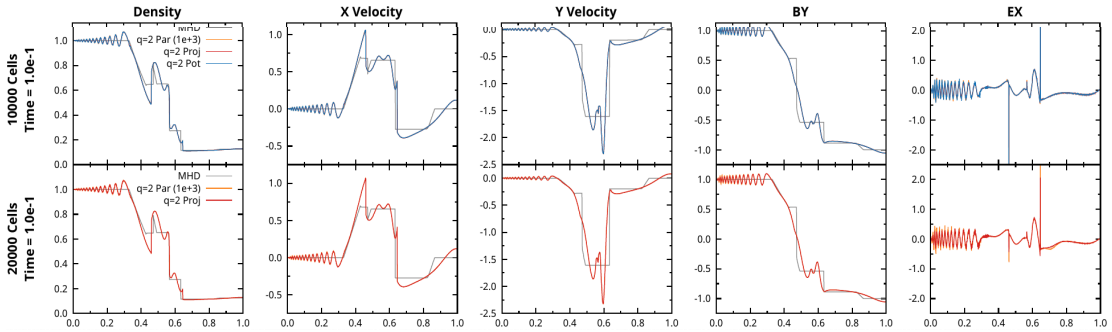

See e.g.
Shumlak et. al.,
Laguna et. al.
Kumar et. al.,
Abgral et. al.

Resolved for MHD scales,
under-resolved for two-fluid scales,
Brio-Wu Problem
Ideal shock MHD limit:

$$\hat{\mu} = 10^{-3}; \hat{\lambda}_D = 10^{-2}; \hat{r}_L = 10^{-4}$$

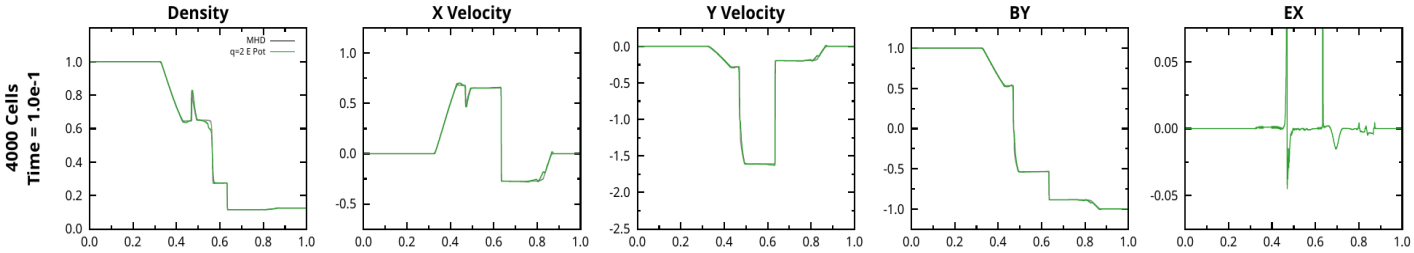

Two-fluid GEM Challenge Benchmark Problem

Current (z)

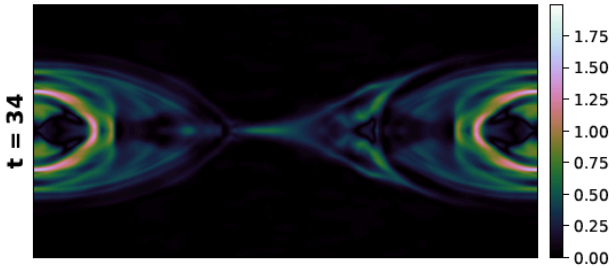

Ion Density

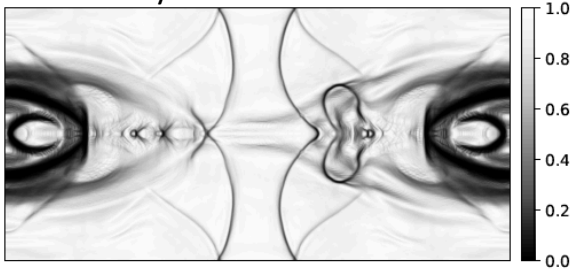

Evolution of Reconnected Flux

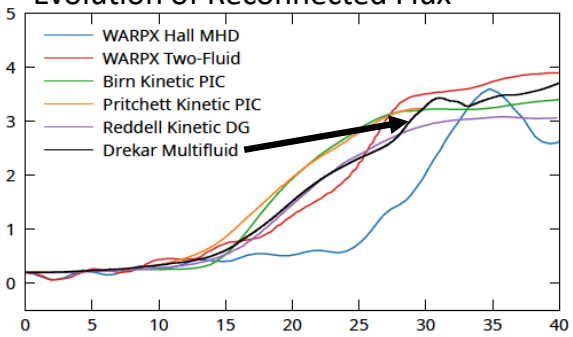

A Tokamak Related Preliminary Example

Tokamak Disruption Simulation (TDS) Center SciDAC-4 Partnership (OFES/ASCR)

<u>Computational Goal</u>

Develop and evaluate advanced hierarchy of plasma physics models and solution methods to understand disruption physics and explore mitigation strategies.

Attempt is to achieve temperature of ~100M deg K (6x Sun temp.),
Energy confinement times O(1) min. is desired.

- **Plasma instabilities can cause break of confinement, huge energy loss, and discharge very large electrical currents (~20MA) into structure.**

- **ITER can sustain only a limited number of disruptions, O(1 – 5) significant instabilities.**

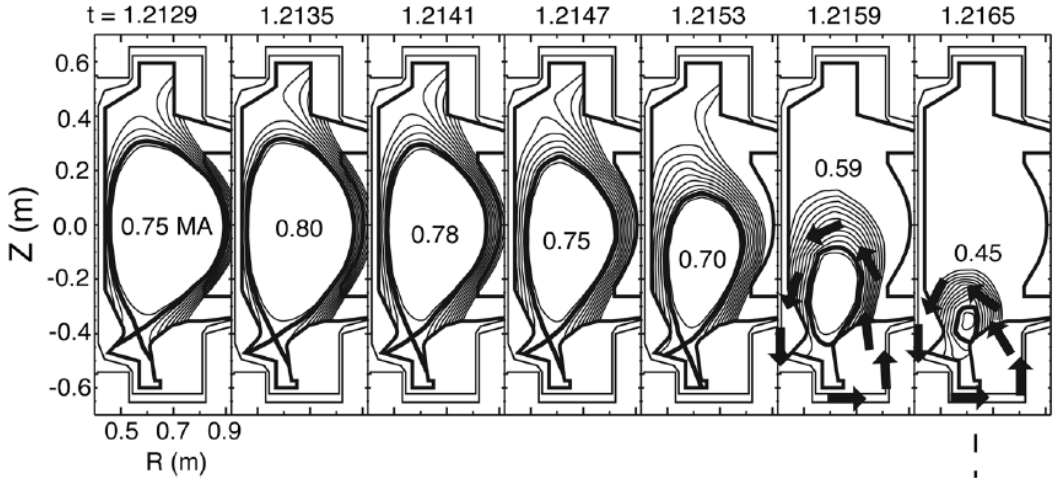

ITER Physics Expert Group on Disruptions,
Nucl. Fusion 39, 2251 (1999).

Preliminary Soloveev MHD Equilibrium Nonlinear Disturbance Saturation.

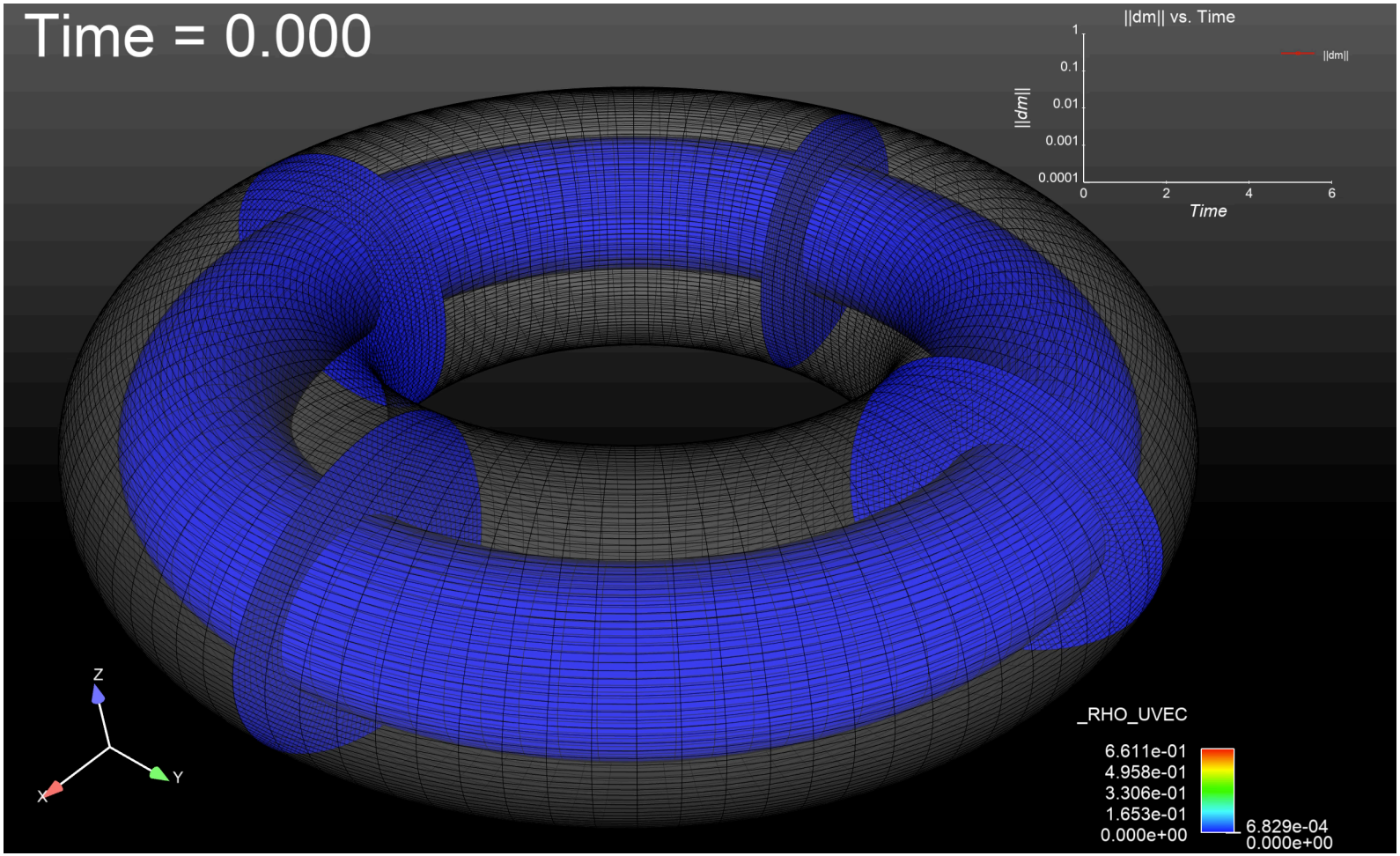

Kink and Interchange Instability.

Drekar

Disruption is a prompt termination of a plasma confinement in a tokamak and can be a showstopper for ITER. Mitigate to control thermal and current quench evolution.

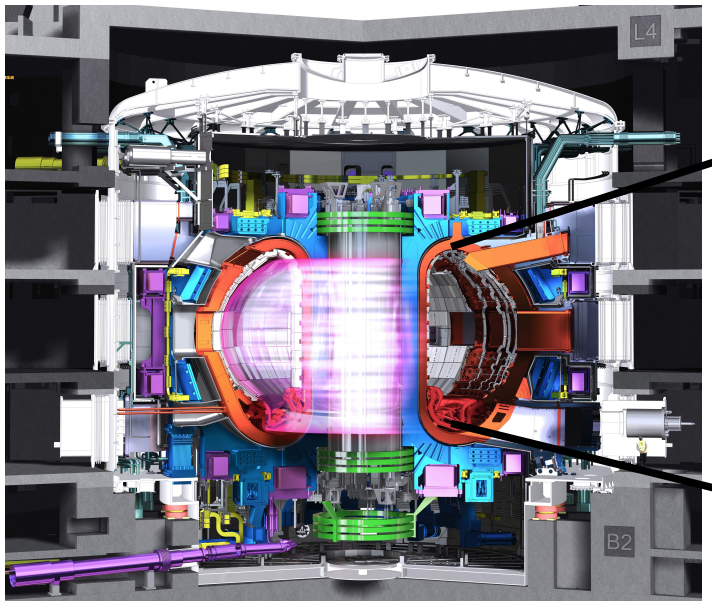

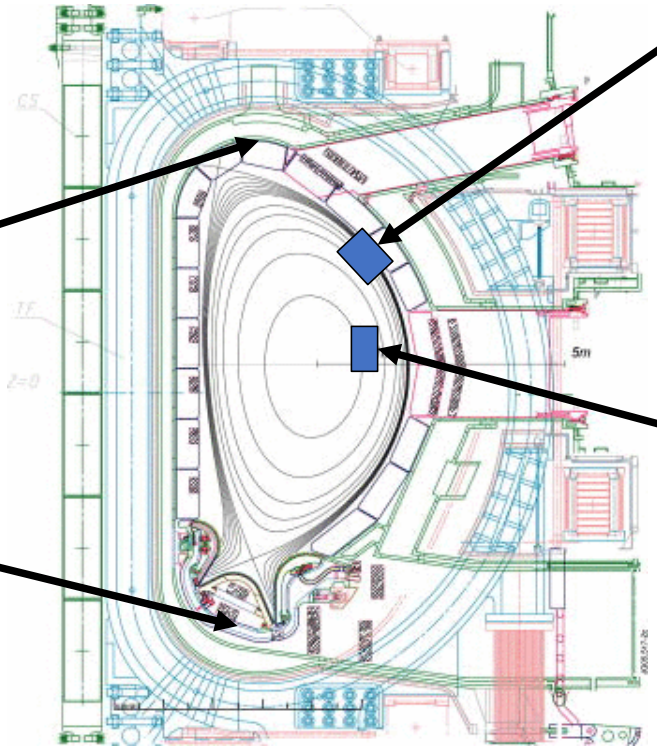

ITER Project: *https://www.iter.org/*

Preliminary Models of Gas Injection for Disruption Mitigation

Dynamics of Neutral Gas Jet Injection at an angle wrt B Field

- Hydrodynamics of jet
- Collisional effects
- Ionization/recombination
  - E field interactions for charged species
  - Interactions with B field for charged species

Gas Injection Assumed Distribution at time t= 0 for Neutral Gas Core Inside Separatrix

- Hydrodynamics of neutral core expansion
- Collisional effects
- Ionization/recombination
  - E field interactions for charged species
  - In 2D,3D interactions with B field for charged species

DOE Advanced Scientific Computing Research (ASCR) / Office of Fusion Energy (OFES)
SciDAC Partnership: Tokamak Disruption Simulation (TDS) Project

Tokamak Disruption Simulation Project (Mitigation with introduction of neutral gases to dissipate runaway electron energy)

- Initial ~fully ionized Deuterium plasma at n ~ 10^{19} - 10^{20} 1/m^3, T = 1 M K
- Neutral gas (H^0, D^0 ,He^0, Ne^0, Ar^0) introduced at n ~ 10^{22} - 10^{24} 1/m^3, T = 1000 K

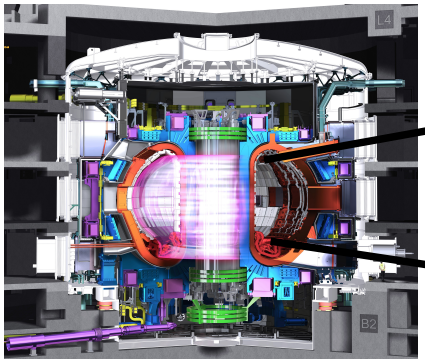

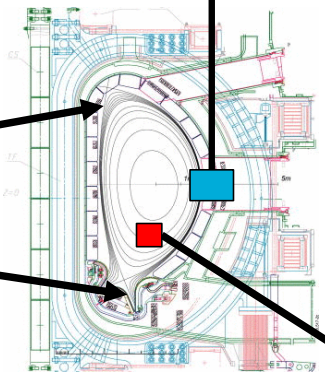

E.g. He Neutral Gas Jet Injection from Wall in Edge Type Region; D^+ Core ~ 10M K $(\mathbf{u} \perp \mathbf{B})$

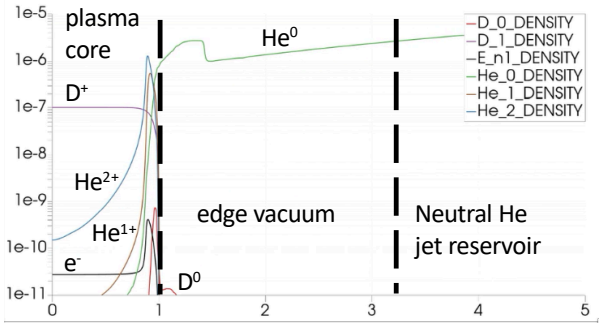

E.g. Ar Neutral Gas Expansion (e.g. post pellet injection) in Core Type Conditions; D^+ Core ~ 10^{20} (1/m^3), 1M K $(\mathbf{u} \parallel \mathbf{B})$

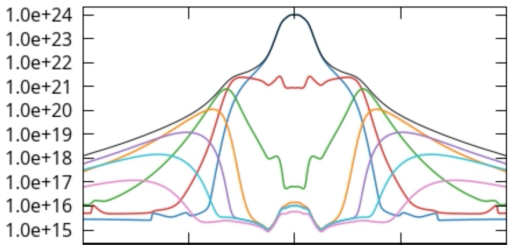

(Ar Neutral + 6 charge levels; 56 PDEs)

Proof-of-principle 1D He Jet injection into static (D^+,e^-) Plasma Core

Drekar: He injection (3e+21 1/m³)
Ionization/recombination and
collisions (no C-X, no line radiation): 10 ms simulation

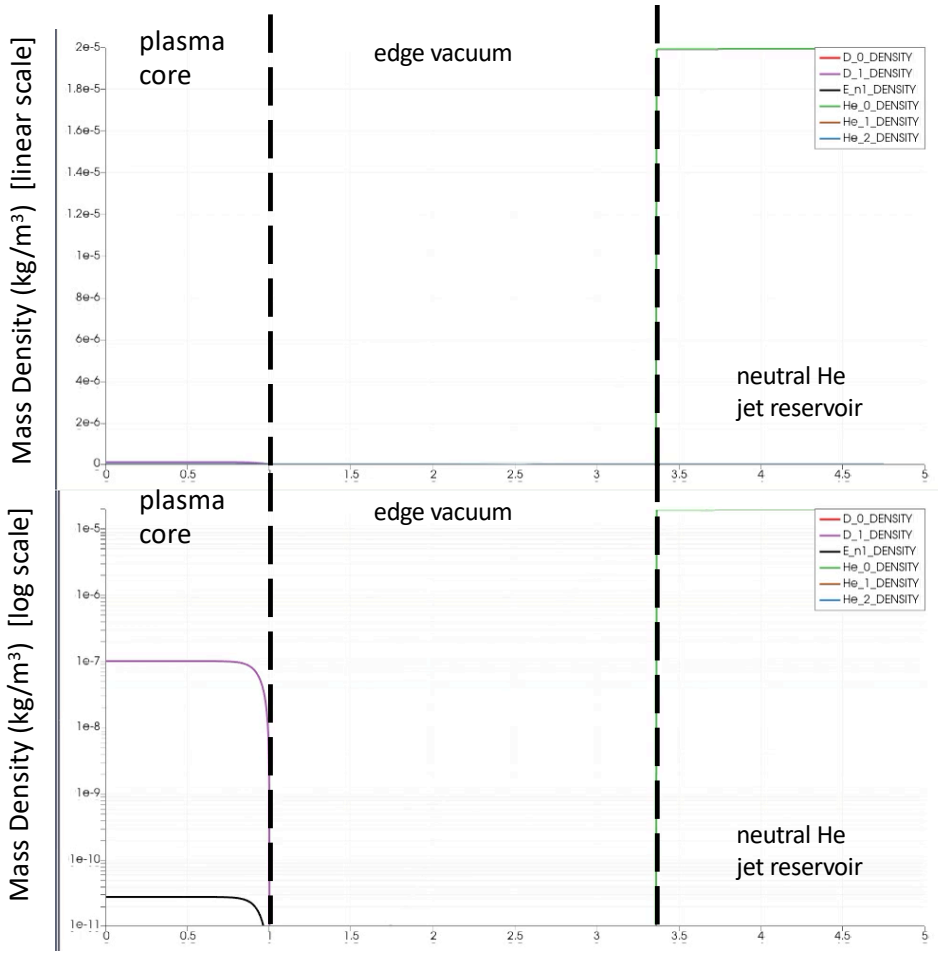

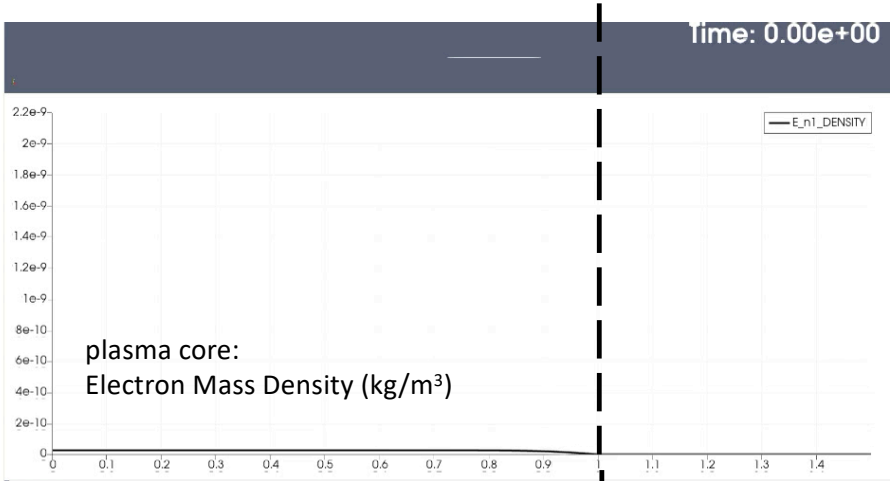

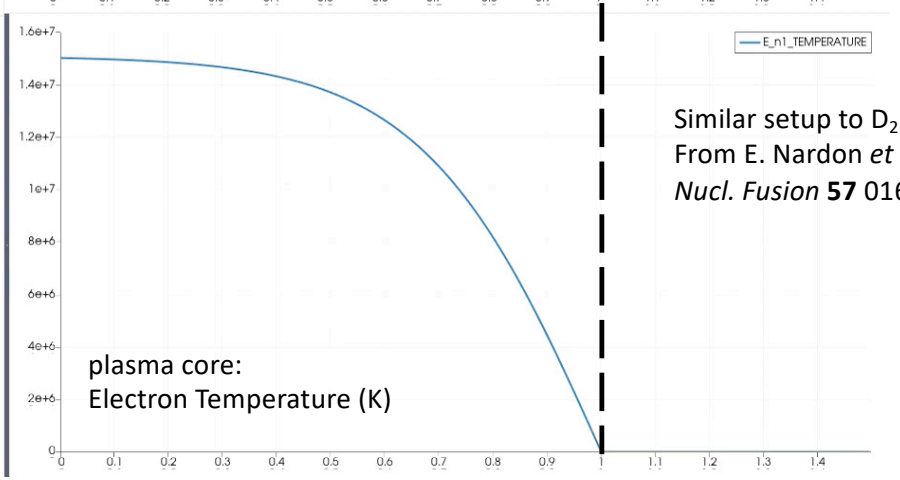

Similar setup to D_2 injection
From E. Nardon *et al* 2017
Nucl. Fusion **57** 016027)

He Jet 3.0e+21

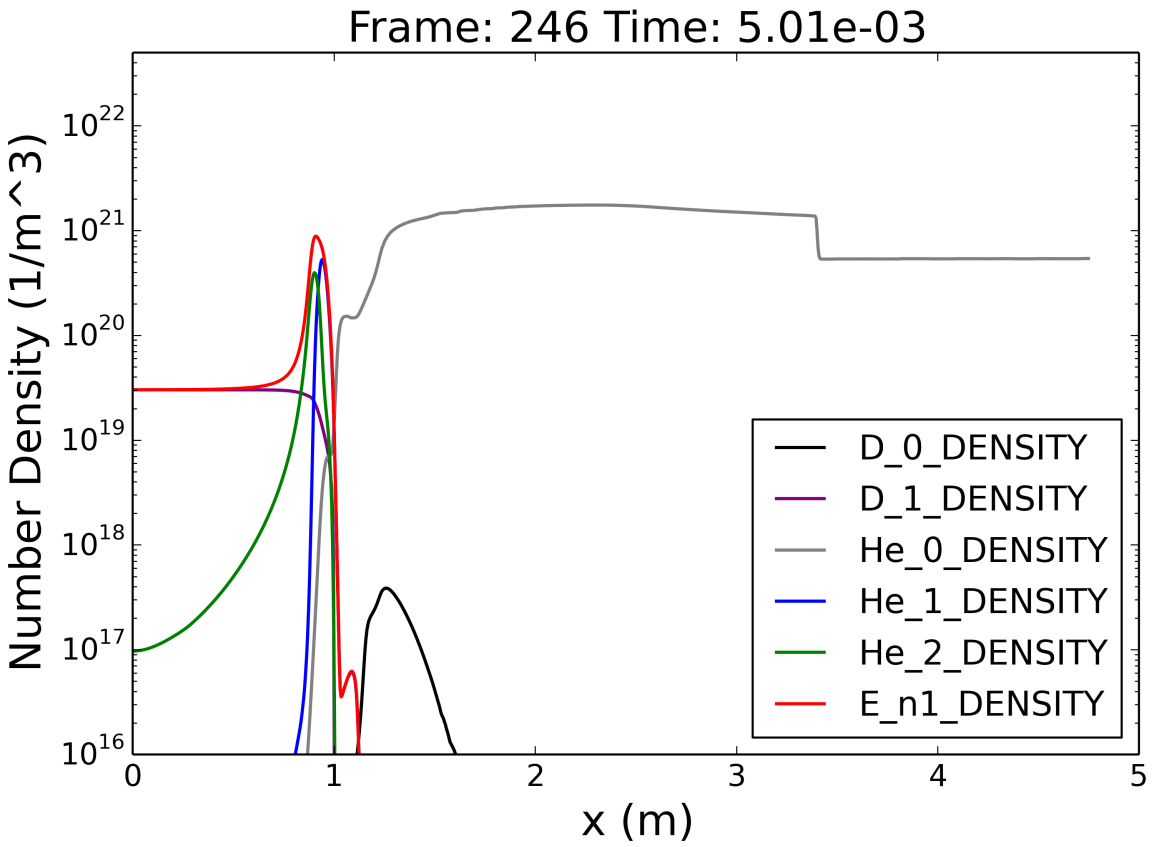
Frame: 246 Time: 5.01e-03
Number Density (1/m^3)
10^{22}
10^{21}
10^{20}
10^{19}
10^{18}
10^{17}
10^{16}
0
1
2
3
4
5
x (m)
D_0_DENSITY
D_1_DENSITY
He_0_DENSITY
He_1_DENSITY
He_2_DENSITY
E_n1_DENSITY

He Jet 6.0e+21

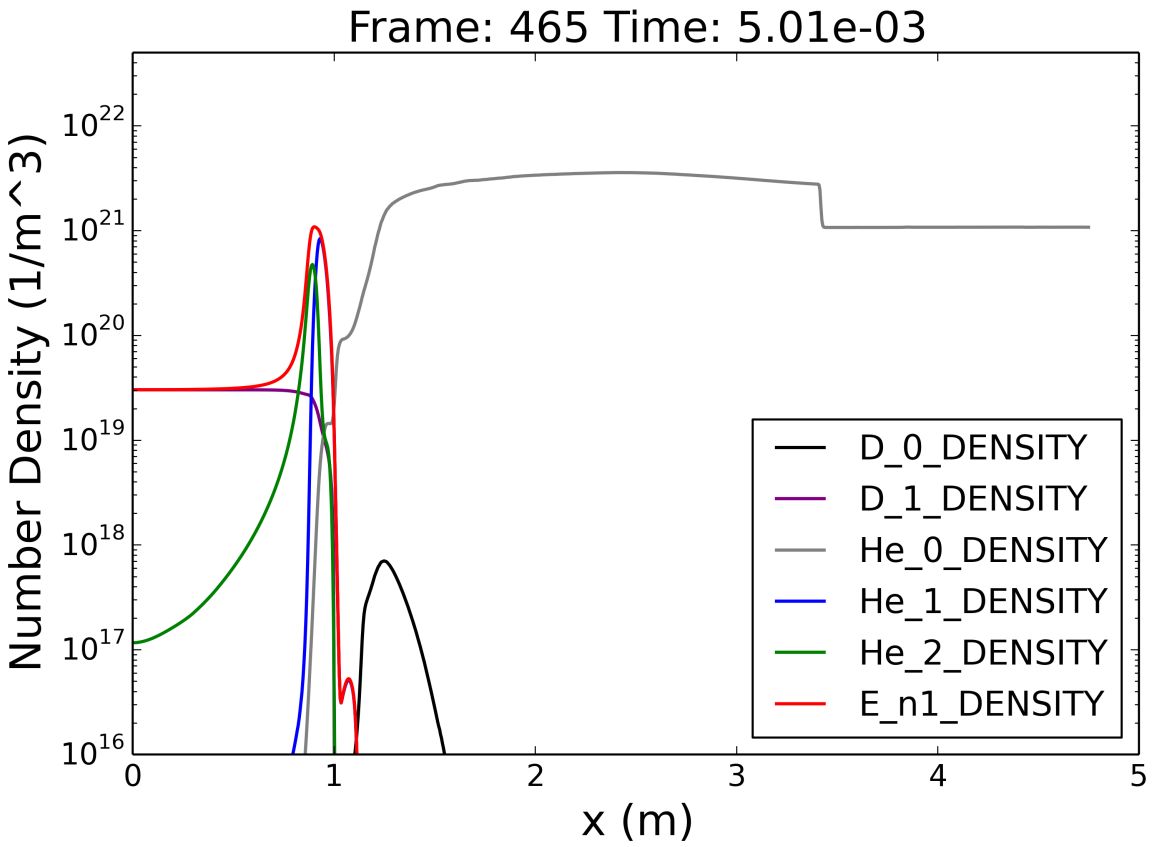
Frame: 465 Time: 5.01e-03
Number Density (1/m^3)
10^{22}
10^{21}
10^{20}
10^{19}
10^{18}
10^{17}
10^{16}
0
1
2
3
4
5
x (m)
D_0_DENSITY
D_1_DENSITY
He_0_DENSITY
He_1_DENSITY
He_2_DENSITY
E_n1_DENSITY

He Jet 1.2e+22

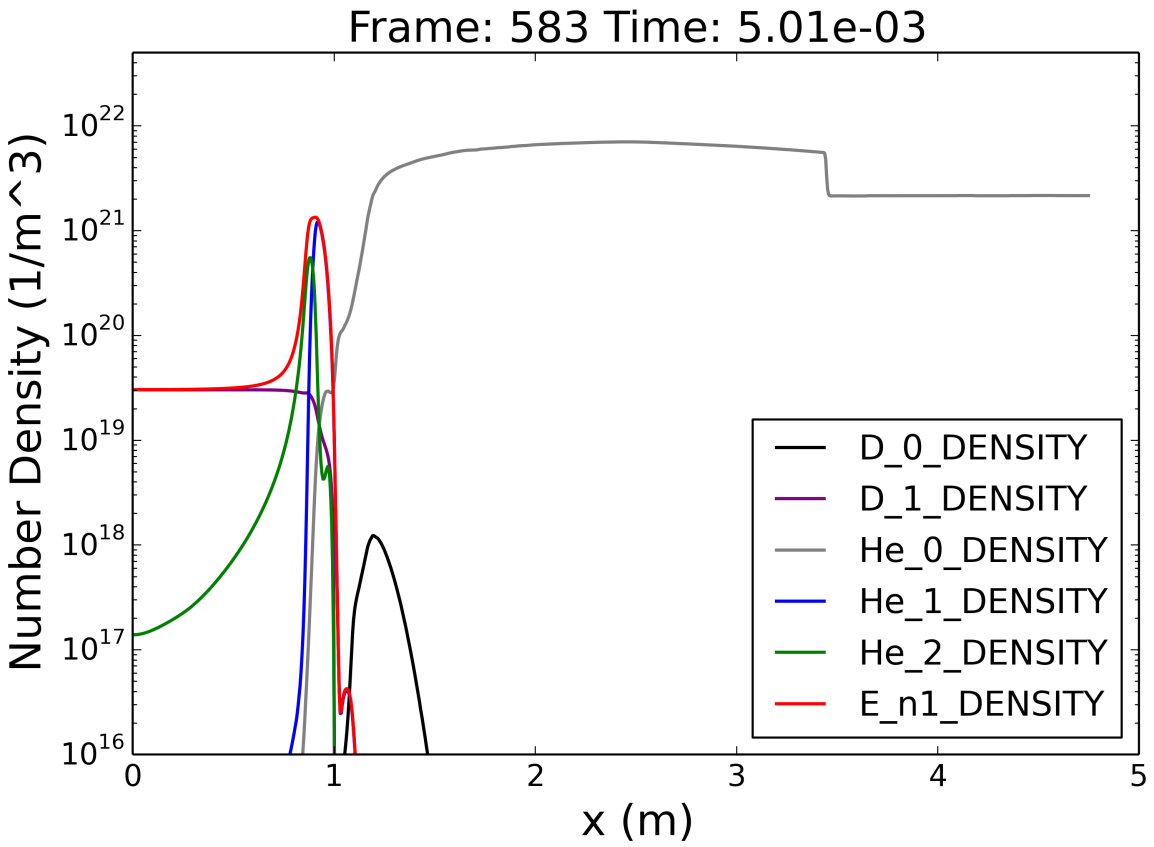
Frame: 583 Time: 5.01e-03
Number Density (1/m^3)
10^{22}
10^{21}
10^{20}
10^{19}
10^{18}
10^{17}
10^{16}
0
1
2
3
4
5
x (m)
D_0_DENSITY
D_1_DENSITY
He_0_DENSITY
He_1_DENSITY
He_2_DENSITY
E_n1_DENSITY

He Jet 2.4e+22

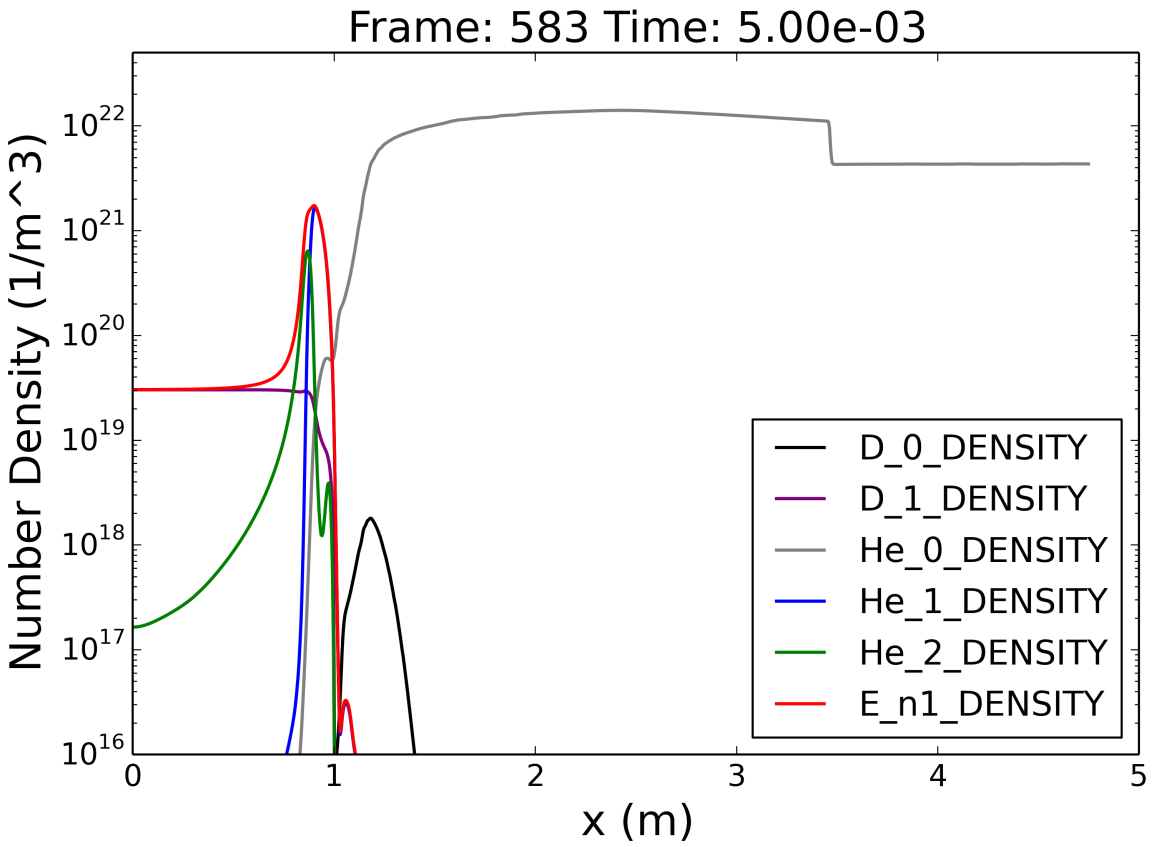
Frame: 583 Time: 5.00e-03
Number Density (1/m^3)
10^{22}
10^{21}
10^{20}
10^{19}
10^{18}
10^{17}
10^{16}
0
1
2
3
4
5
x (m)
D_0_DENSITY
D_1_DENSITY
He_0_DENSITY
He_1_DENSITY
He_2_DENSITY
E_n1_DENSITY

He Jet 3.0e+21

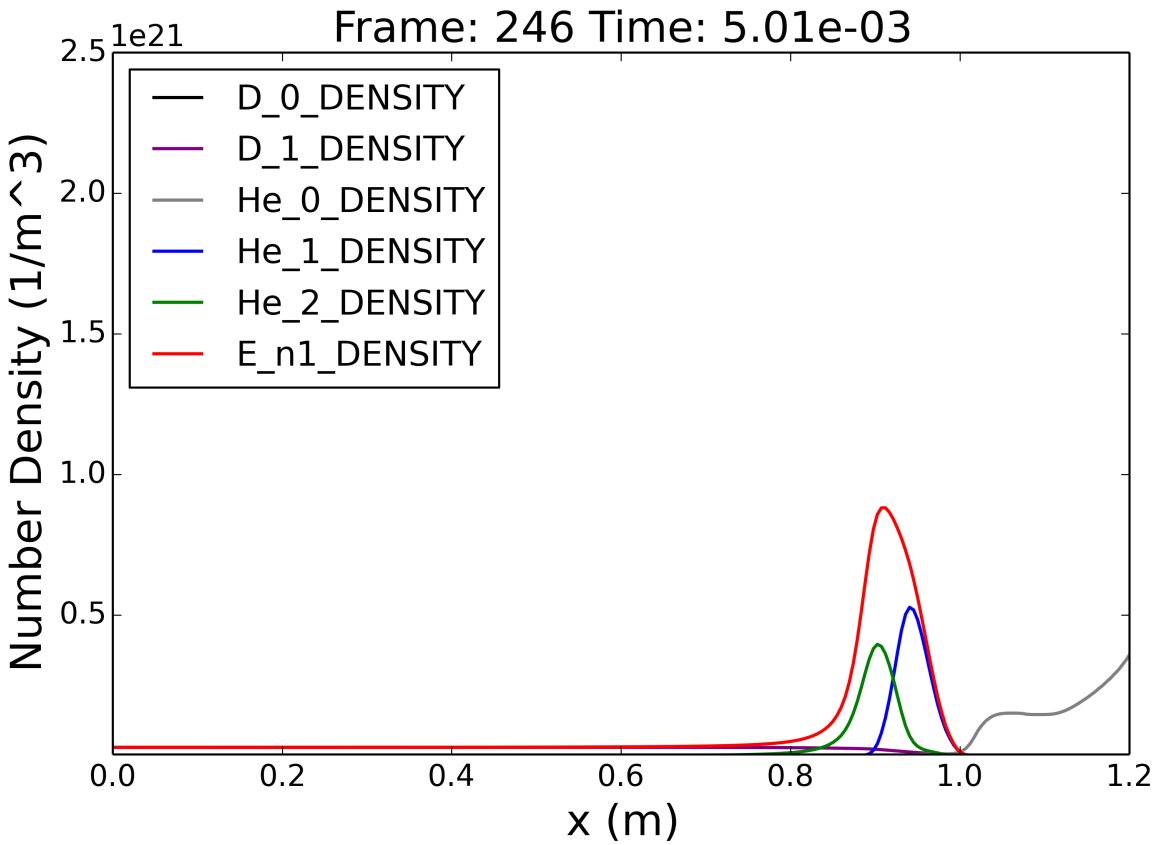
Frame: 246 Time: 5.01e-03
1e21
2.5
2.0
1.5
1.0
0.5
Number Density (1/m^3)
D_0_DENSITY
D_1_DENSITY
He_0_DENSITY
He_1_DENSITY
He_2_DENSITY
E_n1_DENSITY
0.0
0.2
0.4
0.6
0.8
1.0
1.2
x (m)

He Jet 6.0e+21

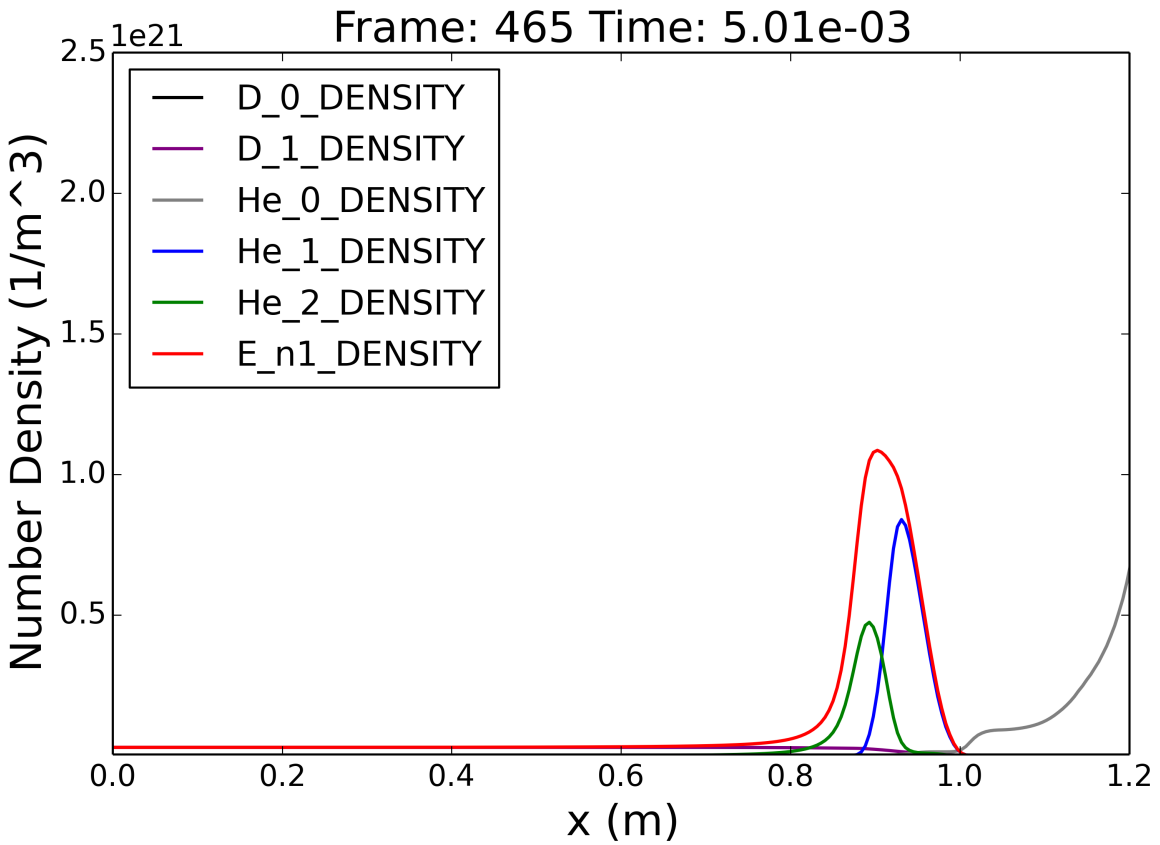
Frame: 465 Time: 5.01e-03
1e21
2.5
2.0
1.5
1.0
0.5
Number Density (1/m^3)
D_0_DENSITY
D_1_DENSITY
He_0_DENSITY
He_1_DENSITY
He_2_DENSITY
E_n1_DENSITY
0.0
0.2
0.4
0.6
0.8
1.0
1.2
x (m)

He Jet 1.2e+22

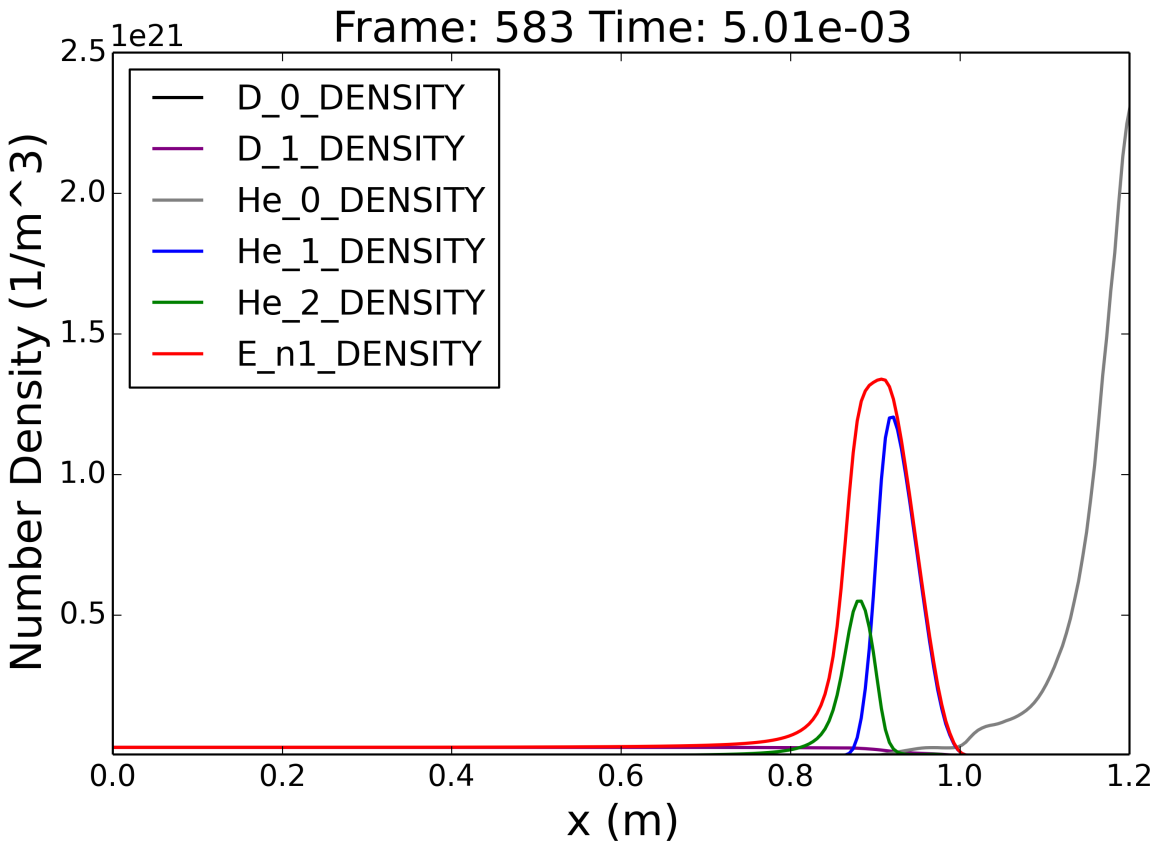
Frame: 583 Time: 5.01e-03
1e21
2.5
2.0
1.5
1.0
0.5
Number Density (1/m^3)
D_0_DENSITY
D_1_DENSITY
He_0_DENSITY
He_1_DENSITY
He_2_DENSITY
E_n1_DENSITY
0.0
0.2
0.4
0.6
0.8
1.0
1.2
x (m)

He Jet 2.4e+22

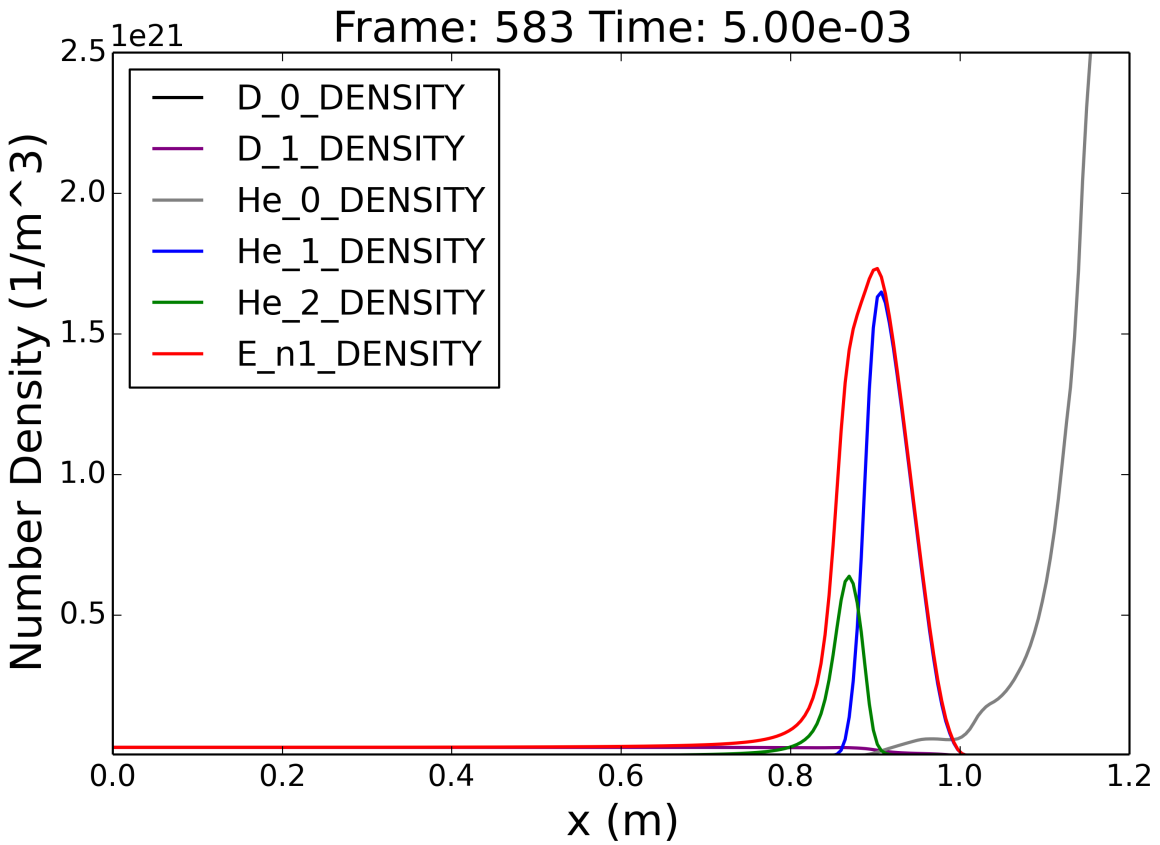
Frame: 583 Time: 5.00e-03
1e21
2.5
2.0
1.5
1.0
0.5
Number Density (1/m^3)
D_0_DENSITY
D_1_DENSITY
He_0_DENSITY
He_1_DENSITY
He_2_DENSITY
E_n1_DENSITY
0.0
0.2
0.4
0.6
0.8
1.0
1.2
x (m)

A Magnetic Implosion Related Preliminary Example

E.g. Multiple-time-scale Multiphysics System: Magnetically-driven Inertial Fusion

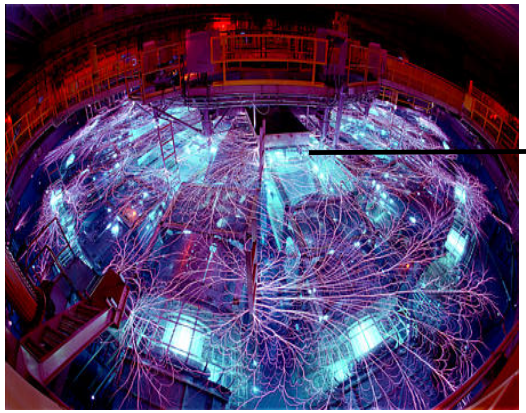

L ~ O(100 m)

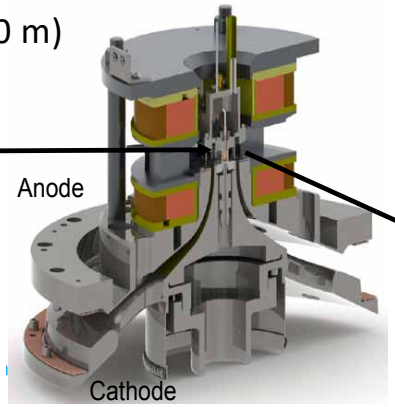

L ~ O(1 m)

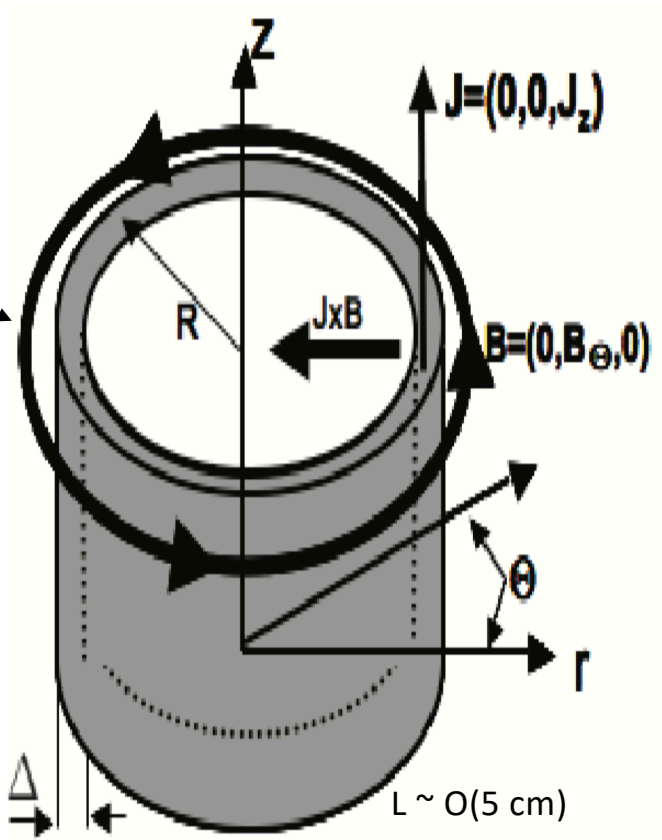

L ~ O(5 cm)

Z Machine (Approximate Ranges)

22 MJ stored energy

100ns current rise time for
26 MA peak electrical current

250 ns plasma shell collapse and stagnation

McBride, Stygar, et. al., A Primer on Pulsed Power and LTD for HEDP App., IEEE Trans. Plasma Sci, 2018

Slutz, Vesey "High-Gain Magnetized Inertial Fusion".
Physical Review Letters. 2012

Sefkow et. al., Design of magnetized liner inertial fusion experiments using the Z facility, PoP 21, 2014

SNL Capabilities: Alegra (Robinson, Garasi, Rider et. al.), Gorgon (Jennings et. al.), Perseus (Martin et. al.), ….

Demonstration of a resistive MHD implosion for a 3D high density gas cylinder.

Simple analytic perfect gas.
Clearly not physical in full range of conditions and the conductivity model is simple analytic.

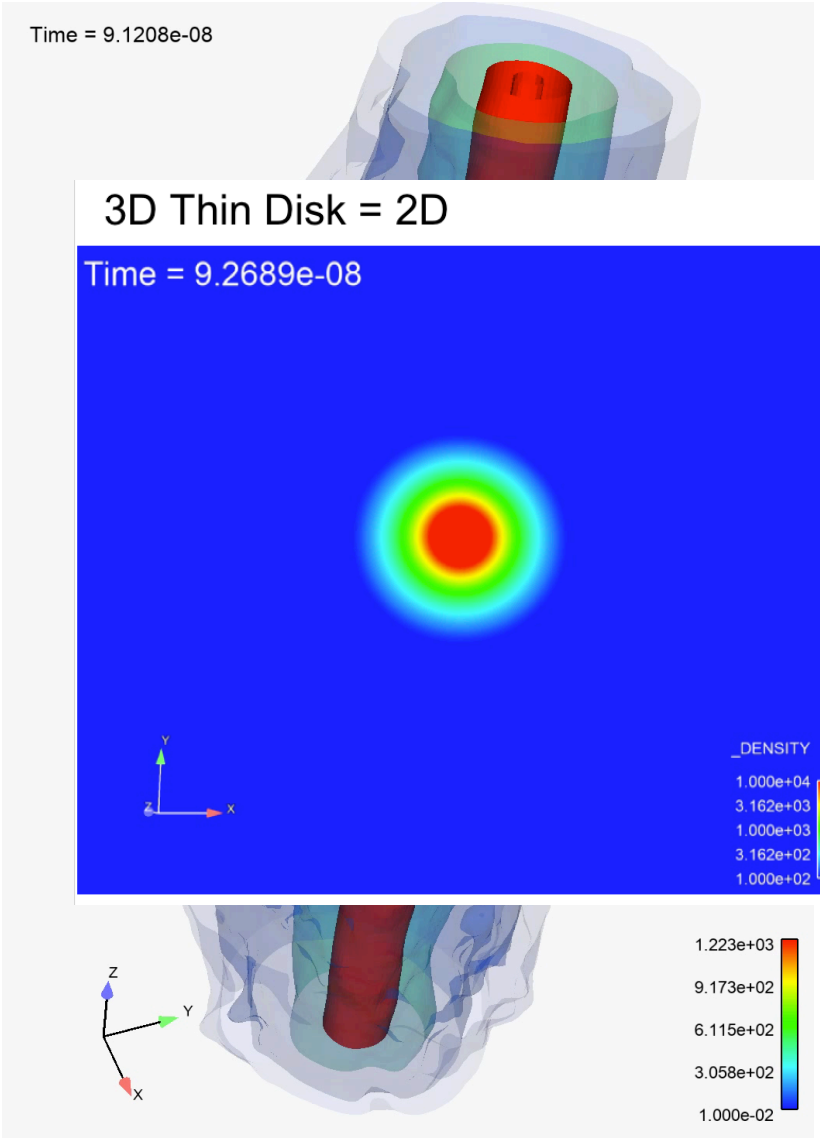

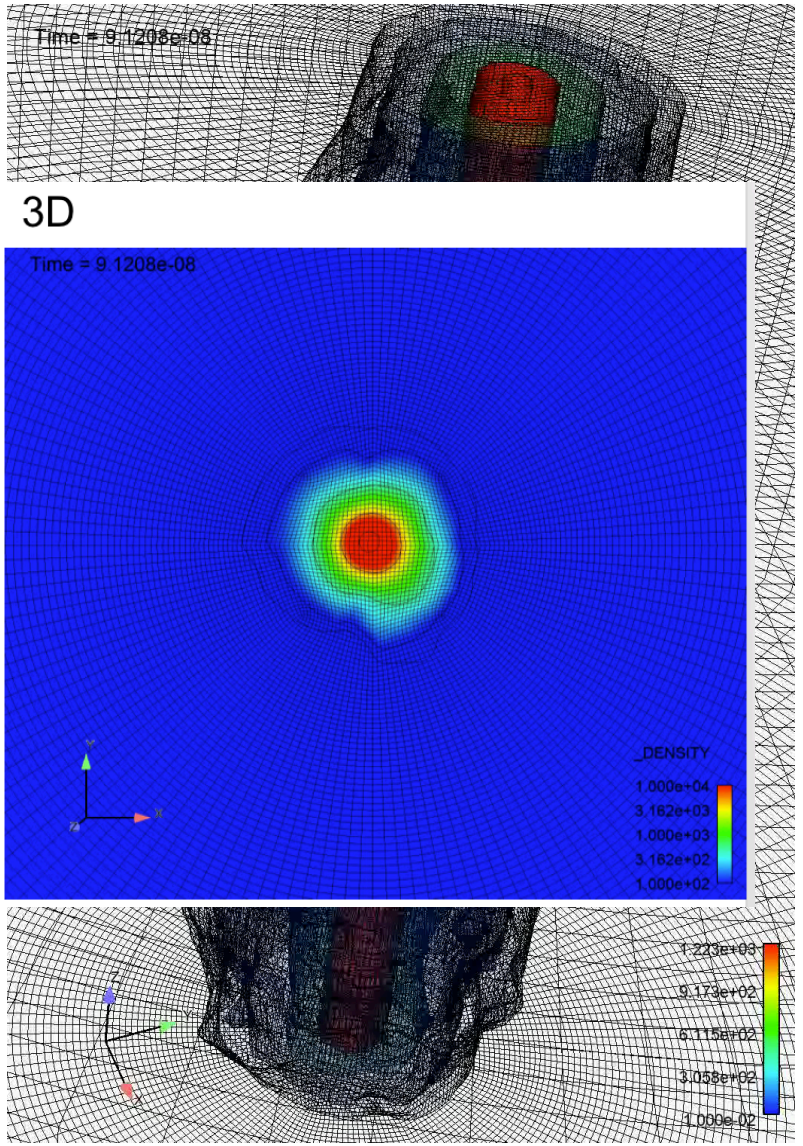

Implicit SSP Dirk22 time integration of 1D Ar gas Z-pinch implosion (Utri / SESAME)

Resistive MHD

EoS from Utri (Ar)
SESAME - LMD elec. conductivities for air

(no radiation losses)

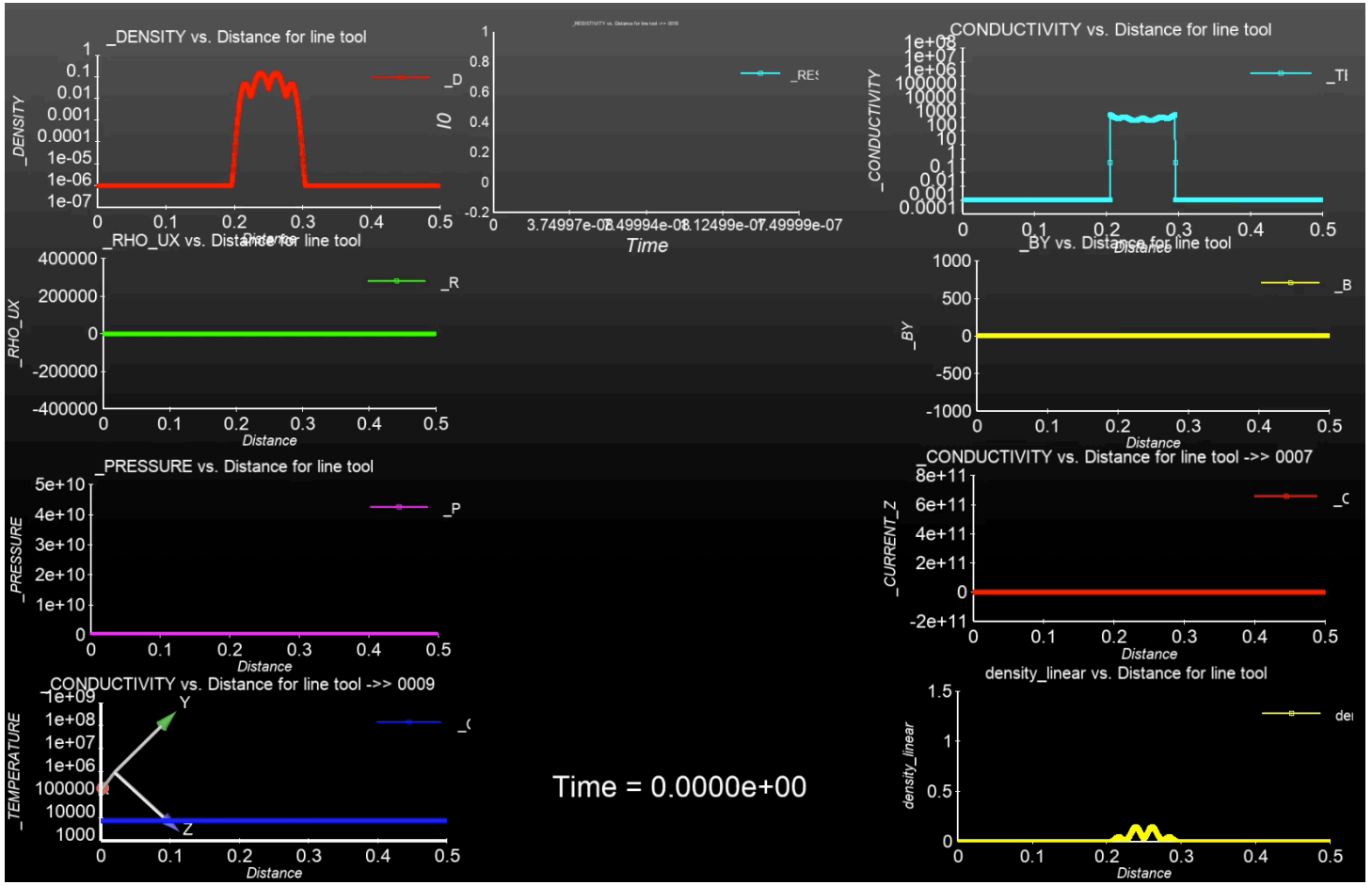

A Proof-of-Principle Demo of Partially-ionized Multifluid Higher Density Ar Gas Puff Z-pinch: $n_{Ar}^0 = 10^{24}$
Includes Collisional/Ionization/Recombination Effects. 10 species {(Ar^{k+},e^-), k = 0, 1, .., 8}

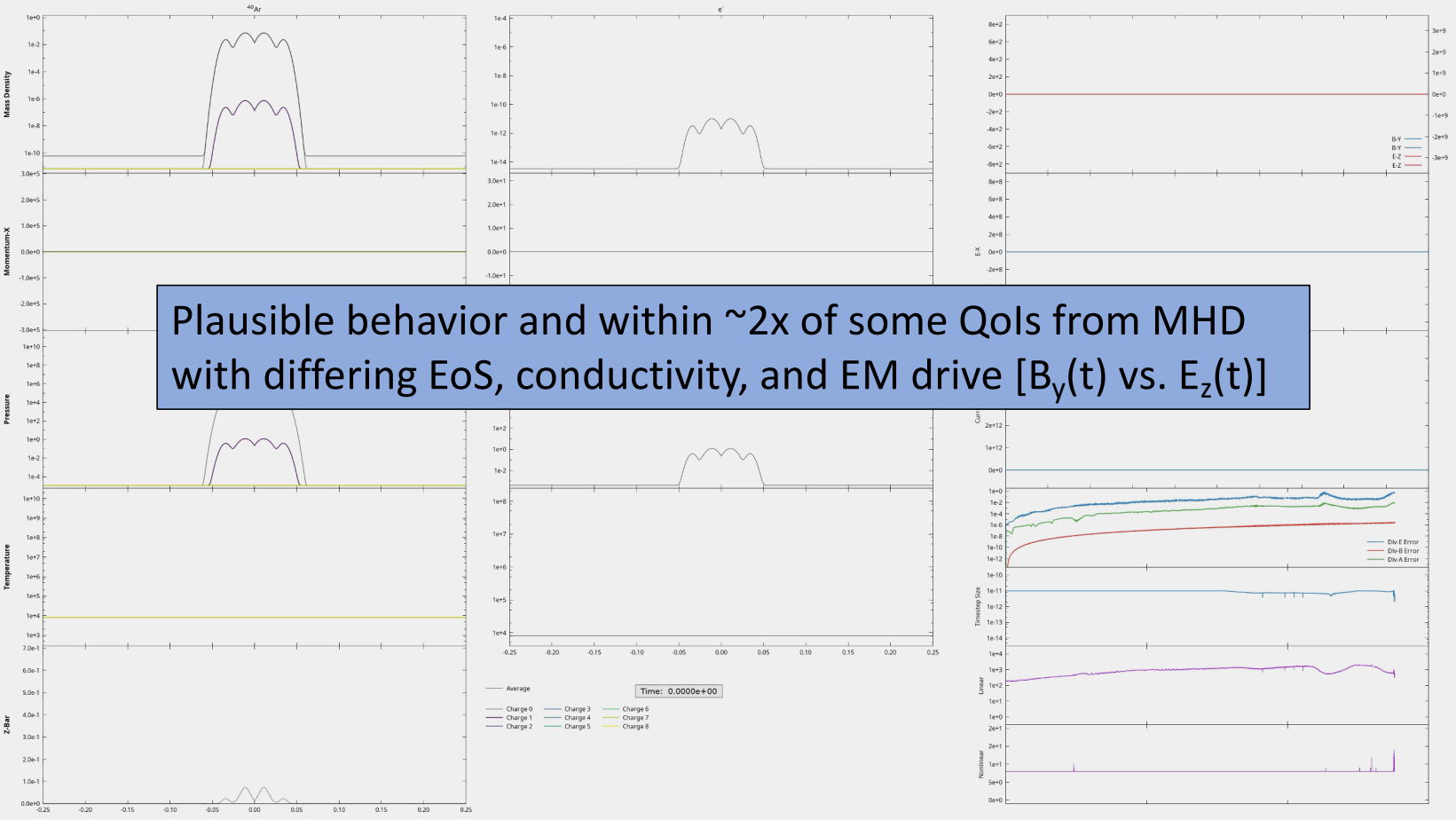

Transverse driving TEM wave (E_z) has 1D geometric factor included: ~20x

Multifluid
EoS Ar ideal gas
- Limited radiation losses
- No higher-density modifications for ionization/recombination

Time step size ~ 2e-11

$$\Delta x|_{min} = 80\mu m$$

$$\tau_c \approx 10^{-13}$$

$$\tau_{\omega p_e} \approx 10^{-13}$$

$$\tau_{\omega c_e} \approx 10^{-13}$$

$$\tau_{V_A} \approx 10^{-13}$$

CFL_c ~10^4 demonstrated on other computations with $\Delta x|_{min} = 1\mu m$

Conclusions

- Robustness, accuracy, flexibility of implicit / IMEX AFC continuous Galerkin discretization is very encouraging.
  - Working towards high-order approximations with AFC FE Bernstein basis. (with D. Kuzmin, H. Hennes, C. Lohmann) and also with HDG (with T. Bui, S. Krishnan)

- Efficiency / scalability of fully-implicit /IMEX parallel NK, physics-based, AMG solvers is encouraging.
  - Physics-based block decomposition and approximate Schur complement preconditioners must have effective approximation of dominant off-diagonal coupling and time-scales in MHD/multifluid plasmas represented.

- Implicit AFC multifluid EM plasma model has demonstrated
  - Robust / and quantitatively reasonable solutions to
    - Challenging benchmark problems (electrostatic shock tube (Sod type), EM shock tube (Brio-Wu type), GEM Challenge, etc.)
    - Solution of implicit full multifluid EM plasma model in ideal shock-MHD asymptotic limit for MHD scales
  - Encouraging preliminary application to
    - MCF: Tokamak disruption mitigation (gas injection)
    - MIF: Ar gas-puff Z-pinch
  - Next steps: Comprehensive convergence results and some validation against experiments

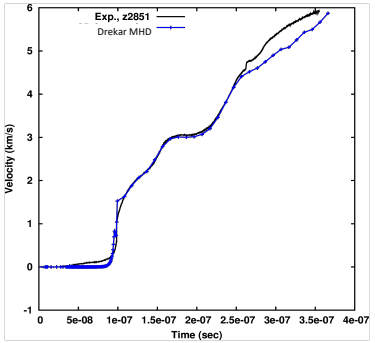

1D Al Flyer Plate VISAR Experiment. vs. MHD Sim.

The End.

Extra slides.

Impact of MHD model assumptions in comparison with multi-fluid 5-moment plasma system models

Resistive MHD (assumptions)	**Multi-fluid EM Plasma Model**
Single ion momentum, continuity eq.	• Include electron, ions, neutrals • Ionization / recombination / charge-exch. • Collisional effects between species
Quasi-neutrality	• Charge separation effects • Sheath formation on surfaces
High plasma frequency	• Plasma oscillations can be resolved
Small (negligible) ion inertial length	• Includes Hall dynamics
Collision dominated Ohm's law	• Electron dynamics included
Low frequency Maxwell equations	• Light wave can be resolved • Propagation of EM waves • Interacting EM waves and plasmas

3D thin Disk = 2D liner compression proof-of-principle

Demonstration of a resistive MHD implosion for comparison with multifluid plasma. 1st step.

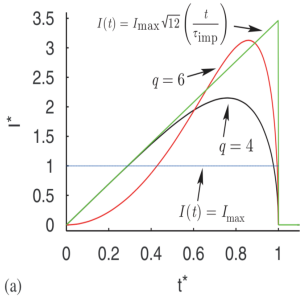

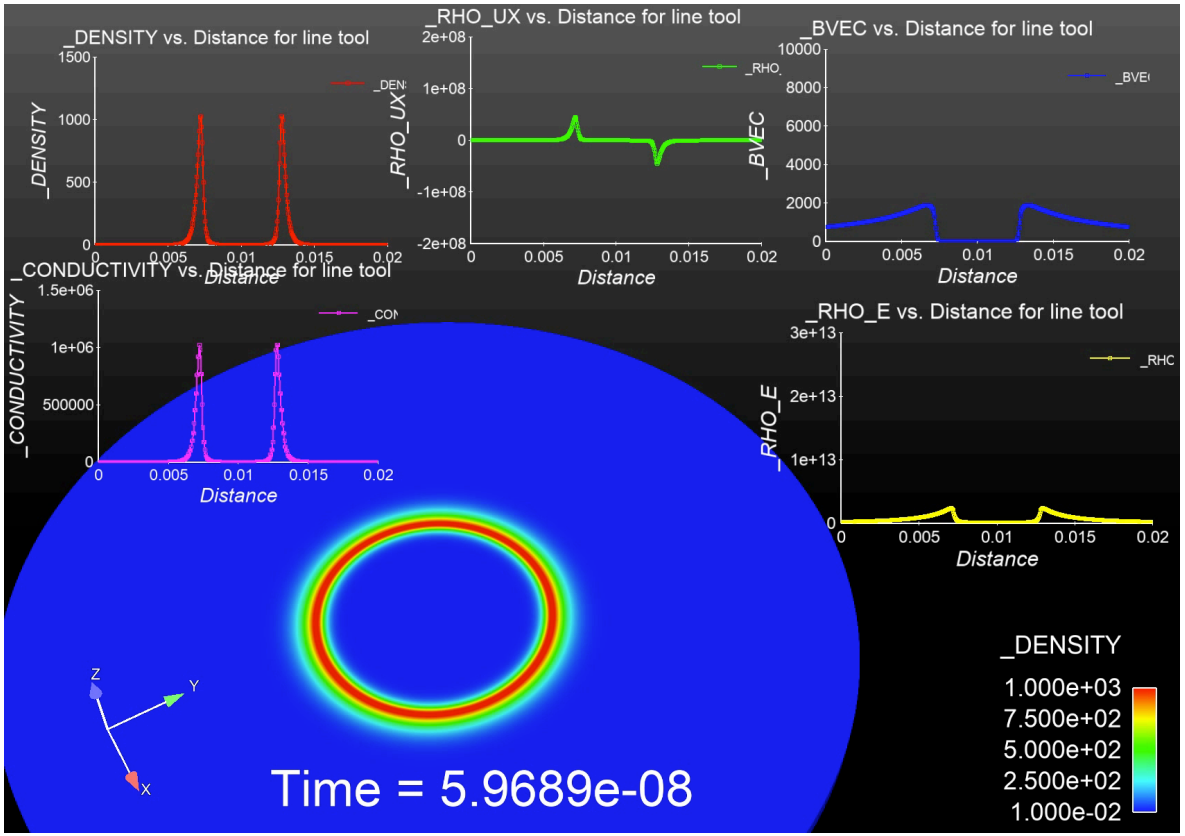

Z-pinch prototype implosion (peak ~60MA, with and without $B_Z^0 = 10T$ $\tau_{imp} \approx 100ns$. Single Material "Ideal Gas", Next step Al with UTRI in progress). Currently LLF bound low-order method, next AFC.

Implicit SSP Dirk22 time integration of 1D Ar gas resistive MHD Z-pinch implosion (ideal gas)

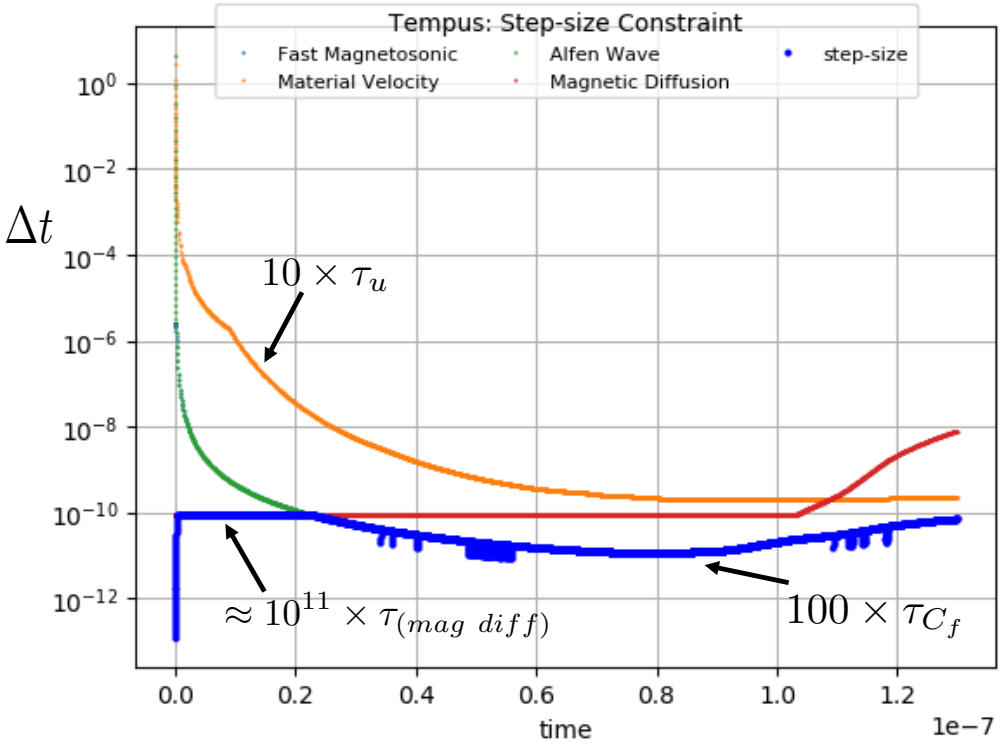

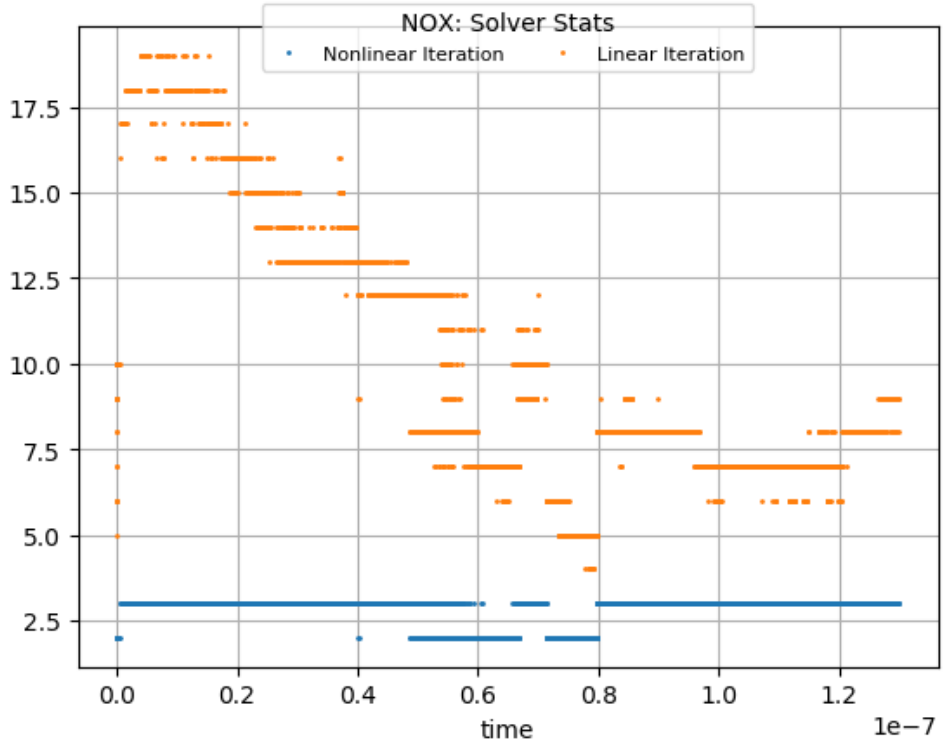

More detail on the AFC element correction factors and construction from nodal variation limiters

$$\mathbf{M}_L \frac{d\mathbf{U}}{dt} + \mathbf{K}(\mathbf{U}) + \mathbf{B}_{\mathbf{\Gamma}}(\mathbf{U}) + \mathbf{D}(\mathbf{U})\mathbf{U} - \sum_e \alpha_e \mathbf{F}^{(\mathbf{e})} = \mathbf{0}$$

$$\alpha_e \in [0, 1]$$

Element correction factor blends low-order ($\alpha_e = 0$) with high-order ($\alpha_e = 1$)

Constructed from nodal variation limiters*.

where $\mathbf{F}^{(e)} = (\mathbf{M}_L^{(e)} - \mathbf{M}_C^{(e)})\dot{\mathbf{U}}^{(e)} + \mathbf{D}^{(\mathbf{e})}(\mathbf{U}^{(\mathbf{e})})\mathbf{U}^{(\mathbf{e})}$

Design properties of element correction factors,

- $\alpha_e = 1$ if the solution is linear
- $\alpha_e = 1$ if the solution is smooth
- $\alpha_e = 0$ in the vicinity of shocks and unresolved steep fronts
- $\alpha_e = 0$ if the solution is a local max/min at unphysical oscillation

Linearized hyperbolic system
*Local Extremum Diminishing (LED) for characteristic variable formulation**. Consistency of first order method:

**Kuzmin et. al. FCT books 2005, 2012; CMAME 2017;*
**Mabuza et. al., JCP 2018, 2020;*

More detail on the AFC element correction factors and construction from nodal variation limiters

Element-wise limiter α_e calculation (Kuzmin, Basting and S , 2017, CMAME):

- Construct a linearity preserving nodal limiter :
  - $\Phi_i(u_i - u_j)$ depends continuously on u_j, $j \in \mathcal{N}(i)$.
  - $\Phi_i(u_i - u_j) = 0$ at a local maximum and local minimum.
  - $\Phi_i(u_i - u_j) = (u_i - u_j)$ if u_h is linear on $\Omega_i = \text{supp}\{\phi_i\}$.

$$\Phi_i^u = 1 - \left[\frac{\left| \sum_{j \neq i} \beta_{ij}(u_j - u_i) \right| + \epsilon}{\sum_{j \neq i} \beta_{ij} |u_j - u_i| + \epsilon} \right]^q,$$

  where $\beta_{ij} \geq 0$ such that $\sum_{j \neq i} \beta_{ij} \boldsymbol{g}_i \cdot (\boldsymbol{x}_j - \boldsymbol{x}_i) = 0$, $q = 10$, and $\epsilon = 1 \times 10^{-16}$.

- Element-wise limiter:

$$\alpha_e^u = \min\{\Phi_i^u\}.$$

- Synchronized limiter:

$$\alpha_e = \min\{\alpha_e^\rho, \alpha_e^{\rho p}\}, \text{ OR } \alpha_e = \min\{\alpha_e^\rho, \alpha_e^s\}, \text{ where } s = \log p - \gamma \log \rho.$$